IMAGING OF INDIRECT CAROTID CAVERNOUS FISTULA COMPARING ADVANCED MRI SEQUENCES WITH DIGITAL SUBTRACTION ANGIOGRAPHY

THESIS

SUBMITTED IN PARTIAL FULFILLMENT FOR DEGREE OF

DM NEUROIMAGING AND INTERVENTIONAL NEURORADIOLOGY

(2017-2019)

OF

THE SREE CHITRA TIRUNAL INSTITUTE FOR MEDICAL SCIENCES AND TECHNOLOGY, TRIVANDRUM, INDIA

DR. SATHISH K

DEPARTMENT OF IMAGING SCIENCES & INTERVENTIONAL RADIOLOGY
SREE CHITRA TIRUNAL INSTITUTE FOR MEDICAL SCIENCES AND TECHNOLOGY, TRIVANDRUM, INDIA

SREE CHITRA TIRUNAL INSTITUTE FOR MEDICAL SCIENCES AND TECHNOLOGY, TRIVANDRUM, INDIA

CERTIFICATE

*This is to certify that the work incorporated in this thesis titled **"Imaging of Indirect Carotid Cavernous Fistula Comparing Advanced MRI Sequences with Digital Subtraction Angiography"** for the degree of **DM NEUROIMAGING AND INTERVENTIONAL NEURORADIOLOGY** has been carried out by **DR. SATHISH K** under our supervision and guidance. The work done in connection with this thesis has been carried out by the candidate himself and is genuine.*

Dr. Santhosh Kumar K
Associate Professor
Principal Guide

Dr. Jayadevan ER
Additional Professor
Co- Guide

Dr. Bejoy Thomas
Professor
Co-Guide

Dr Kesavadas C
Professor & HOD
Department of Imaging Sciences and Interventional Radiology,
SCTIMST, Thiruvananthapuram.

DECLARATION

*I hereby declare that this thesis titled "***Imaging of Indirect Carotid Cavernous Fistula Comparing Advanced MRI Sequences with Digital Subtraction Angiography***" has been prepared by me under the supervision and guidance of Dr.Santhosh Kumar K (Associate Professor) , Dr Jayadevan E R (Additional Professor), Dr Bejoy Thomas (Professor), Department of Imaging Sciences and Interventional Radiology, Sree Chitra Institute for Medical Sciences and Technology, Trivandrum.*

Date: *(Dr Sathish K)*

Place: Thiruvananthapuram

ACKNOWLEDGEMENT

- I am deeply indebted to my teachers & guides especially Dr. Santhosh Kumar K, Dr. Jayadevan E R and Dr. Bejoy Thomas, of Department of Imaging Sciences and Interventional Radiology, for their constant unwavering support, insightful criticism, expert supervision and immense patience throughout this study.

- I am profoundly grateful to Dr. Kesavadas C and Dr.Kapilamoorthy TR, for their omnipresent support and guidance during this tenure.

- I would specially like to acknowledge my gratitude to my past and present colleagues and the technologists of the Department of IS and IR and the advanced radiology technology trainees of the department, Mr.Sajith, Mr.Jithin, Mr.Arun, Miss.Anusree for their valuable assistance at all times during the course of this study.

- I would also like to extend my heartfelt gratitude to my family for being immensely supportive all through my endeavours. I could not have achieved what I have without their prayers, love, and support.

- Finally, I am eternally grateful to all my patients & their relatives who have been very understanding and generous with their cooperation all through the study.

CONTENTS

INTRODUCTION:

Carotid-cavernous fistulas (CCFs) are abnormal arteriovenous communications either directly between the internal carotid artery (ICA) and the cavernous sinus or between the dural branches of the internal and external carotid arteries. Several classification schemes have categorized CCFs according to aetiology (traumatic or spontaneous), hemodynamic features (high versus low flow), or the angiographic arterial architecture (direct or indirect). Direct CCFs usually arise after trauma or a ruptured aneurysm. These fistulae are less likely to resolve spontaneously and may require intervention if symptomatic. The remaining types are indirect and are best described as dural arteriovenous malformations. Their rate of flow and exact aetiology are variable. They have been associated with pregnancy, cavernous sinus thrombosis, sinusitis, and minor trauma. Most of the patients are managed conservatively and may require intervention if there is any deterioration during follow up. (1)

Intra-arterial digital subtraction angiography (DSA) is the standard of reference for the diagnosis of CSDAVFs. Its high spatial and temporal resolution facilitates the accurate analysis of feeders, venous drainage, and fistula sites. However, DSA is invasive and not without possible complications; morbidity of 0.03% and mortality of 0.06% have been reported for patients undergoing diagnostic cerebral angiography(2,3). Therefore, a noninvasive, reliable method is needed for the appropriate selection of patients with CSDAVF with high risk (aggressive symptoms), exclusion of patients with CSDAVF considered benign and for follow-up. Carotid-cavernous fistula descriptions are with type, location, laterality, size of fistula, feeding arteries, draining veins and cortical venous reflux.

Recently few studies are published on cranial dural arteriovenous fistulas (cDAVF) comparing the efficacy of advanced vascular MR imaging with DSA. Comparison of 3D-TOF (3T) with DSA in the evaluation of intracranial DAVF showed good intermodality agreement in the gross characterization of DAVF(4). Few studies showed SWI can reliably detect the fistulous point, presence of cortical venous reflux in cases of DAVF and also helps in differentiating nidus from haemorrhage and calcification in cases of brain AVM(5,6).

Susceptibility-weighted angiography (SWAN) is a new 3D T2*- based gradient-echo sequence generating several echoes that are read out at different TE times, allowing high-resolution visualization of both cerebral veins and arteries. SWAN sequence has a potential role for the diagnosis of intracranial DAVF in visualising intracranial arteriovenous shunt(7).

Silence Magnetic resonance angiography is a relatively new technique available in 3.0 Tesla Magnetic Resonance scanners. The advantages of this arterial spin labelling (ASL) based ultra-short echo-time technique is that it is less affected by susceptibility effects and has excellent background suppression. Few preliminary studies have found that the vascular anatomy is better depicted on Silence magnetic resonance(8).

To our knowledge, there are no systematic studies on the reliability of unenhanced 3T 3D TOF MRA, Silent MRA and SWAN for assessing feeders, fistula sites, and venous drainage of CSDAVFs. Thus, this intended to study the utility of these noninvasive magnetic resonance angiography techniques to determine the angiomorphology of CCF, in treatment planning and follow up. If found reliable it may supplant DSA in follow up imaging.

HYPOTHESIS:

Advanced MRI and MRA imaging- 3D TOF, SWAN, Silence MRA can reliably help in non-invasive detection and characterization of the indirect Carotid-cavernous fistulas.

AIMS & OBJECTIVES:

- To compare the advanced vascular MRI sequences (3D TOF, SWAN, Silent MRA), in the evaluation of indirect Carotid-cavernous fistulas with Digital subtraction angiography to determine the angiomorphology of CCF.

REVIEW OF LITERATURE:

INTRODUCTION:

A carotid-cavernous sinus fistula (CCF) is an abnormal communication between the cavernous sinus and the carotid arterial system. CCFs can be classified by cause (traumatic vs spontaneous), velocity of blood flow (high vs low flow), and anatomy (direct vs dural, internal carotid vs external carotid vs both). Some fistulas are characterized by a direct connection between the cavernous segment of the internal carotid artery and the cavernous sinus. These fistulas are usually of the high-flow type. They are called direct CCFs and are most often caused by a single, traumatic tear in the arterial wall or at times by the rupture of an intracavernous aneurysm. Other CCFs are dural(1). Many of these lesions are actually congenital arteriovenous fistulas that develop spontaneously, often in the setting of atherosclerosis, systemic hypertension, connective tissue disease, and during or after childbirth(9). Dural CCFs consist of a communication between the cavernous sinus and 1 or more meningeal branches of the internal carotid artery, the external carotid artery or both. Of these, fistulas involving branches from both the internal and external carotid arteries are the most common. These fistulas usually have low rates of arterial blood flow(10).

ANATOMY:

Knowledge of the anatomy of the cavernous sinus is essential for understanding the clinical symptoms of CCFs and the various treatment options. The cavernous sinus comprises a network of venous channels with intervening extravascular space through which the cavernous portion of the ICA and cranial nerve (CN) VI course. The CNs III, IV, and V (first and second divisions) run within the dura of the lateral wall of the cavernous sinus.

The cavernous segment of the ICA invariably gives off a meningohypophyseal trunk, and less frequently, an inferior cavernous sinus artery or inferolateral trunk, the McConnell's capsular artery in a minority of patients, and the ophthalmic artery and/ or the dorsal meningeal artery(11). The meningohypophyseal trunk in turn commonly gives off the following branches: the tentorial artery, inferior hypophyseal artery, and the dorsal meningeal artery.

The venous drainage from the cavernous sinus includes: the superior and inferior ophthalmic veins anteriorly; the superior and inferior petrosal sinuses, pterygoid plexus and clival (basilar) venous plexus posteriorly and inferiorly; and retrograde cortical drainage via the superficial middle cerebral veins, perimesencephalic veins, and cerebellar veins. There are also variable direct venous interconnections between the right and left cavernous sinuses. The pattern of the venous outflow is an important factor in determining the optimal transvenous therapeutic approach to CCFs(12).

ICA and ECA branches relevant for supply of CSDAVF and their main anastomoses to adjacent territories (13)

1. ***MHT***

   Tentorial trunk

   - Medial tentorial artery (to contralateral, lateral tentorial, dorsal meningeal, MMA, ILT)
   - Lateral tentorial artery (to medial tentorial, dorsal meningeal, posterior meningeal, mastoid)

   Dorsal meningeal artery (to contralateral, medial clival, tentorial, MMA, APA)

   Inferior hypophyseal artery (to contralateral, capsular)

   Medial clival artery (to contralateral, dorsal meningeal, medial tentorial)

2. ***ILT***

   Superior ramus (to medial tentorial)

Anterior Ramus

Anteromedial ramus (to deep recurrent ophthalmic)

Anterolateral ramus (to AFR)

Posterior Ramus

Posteromedial ramus (to AMA)

Posterolateral ramus (to MMA)

3. ***Ophthalmic artery***

Anterior ethmoidal arteries

Posterior ethmoidal arteries

Deep recurrent ophthalmic artery (to ILT)

Superficial recurrent ophthalmic artery (to medial tentorial)

Recurrent meningeal artery (to MMA)

Recurrent artery of the foramen lacerum (to APA, ILT, vidian)

4. ***ECA***

Ascending pharyngeal artery

Carotid ramus (to RAFL)

Jugular ramus (to lateral clival)

Hypoglossal ramus (to medial clival)

Maxillary artery

Artery of pterygoid canal (to AMA, APA, C5 segment, RAFL)

Pterygovaginal artery

Middle meningeal artery (to ILT, AMA, OA)

Accessory meningeal artery (to MMA, ILT, medial tentorial)

Cavernous sinus and its main afferent (tributaries) and efferent (draining) veins CS

- ***Afferent veins***

  Orbital veins

    Superior ophthalmic vein

    Inferior ophthalmic vein

    Central retinal vein (to SOV, CS)

  Angular vein (to SOV)

  Superficial middle cerebral vein (SMCV)

  Uncal vein (UV)

  Sphenoparietal sinus (SPPS)

  Intracavernous sinus (ICS)

  Meningeal veins

  Veins of the foramen rotundum

- ***Efferent veins***

  Superior petrosal sinus (SPS)

  Inferior petrosal sinus (IPS)

  Basilar plexus (BP)

  Pterygoid plexus (PP)

  Inferior petroclival vein (IPCV)

  Petro-occipital sinus

  Internal carotid venous plexus

  Foramen ovale plexus (FOP)

  Foramen lacerum plexus

CLASSIFICATION:

Several classification schemes have described CCFs based on their etiology (traumatic or spontaneous), flow rate (high or low), and communication with the internal carotid artery (ICA) (direct or indirect). The most widely accepted classification is that proposed by Barrow and colleagues(1), which categorizes CCFs into four distinct types based on their arterial supply:

Type A: direct communication of the fistula with the ICA

Type B: CCF arterial supply provided by meningeal ICA branches

Type C: CCF arterial supply provided by meningeal external carotid artery branches

Type D: CCF arterial supply provided by meningeal branches of both the ICA and the external carotid artery.

Direct fistulas are characterized by a direct connection between the internal carotid artery (ICA) and the cavernous sinus. They are usually high-flow fistulas. (14).

Dural CCFs typically are low-flow fistulas that consist of communications between the cavernous sinus and cavernous arterial branches. Barrow type B fistulas involve meningeal branches of the ICA, Barrow type C involve external carotid branches, and Barrow type D fistulas include meningeal branches from both the internal and external carotid arteries. Spontaneous dural CCFs are usually type D(15). The artery of the inferior cavernous sinus is the most frequently implicated trunk of the ICA, but dural fistulas also may involve the meningohypophyseal trunk and its branches. The most commonly involved branch of the external carotid artery is the internal maxillary artery, with other implicated branches being the middle and accessory meningeal arteries, ascending pharyngeal artery, anterior deep temporal artery, and posterior auricular artery.

Suh et al(16) (2005) have suggested angiographic differentiation of CSDAVFs into three types:

1. The Proliferative type (PT):

– Numerous arterial feeders to the CS (network)

– Large AV shunt with rapid filling of CS, afferent and efferent veins

– Both CSs completely filled and bulging into the sinus wall

2. The Restrictive type (RT):

– Less arterial feeders than PT, each identifiable

– Obliteration of flow in IPS, increased flow in

SOV and cortical veins

– Less AV shunt than in PT

– CS margins less well defined (loss of normal contour)

3. The Late Restrictive type (LRT):

– Few arterial feeders

– With sluggish retrograde venous flow

– Constrictive changes of the veins

– CS stasis

In 2015, Thomas et al(12) proposed a new classification system for CCFs based on venous drainage, which also significantly influences clinical presentation and in many cases guides therapeutic intervention. This classification system specifies 5 types of CCFs:

Type 1—posterior/inferior venous drainage only.

Type 2—posterior/inferior and anterior venous drainage.

Type 3—anterior venous drainage only.

Type 4—retrograde cortical venous drainage.

Type 5—direct ICA-cavernous sinus fistulae corresponding to the type A Barrow classification.

Kiyouse et al. categorized CSDAVF into four groups as posteromedial, posterolateral, medial and lateral subtypes, of which posteromedial type was the commonest. For successful embolization of the CSDAVFs, it is important to know the location of the shunted pouch, as it allows the reduction of shunt flow using a small number of coils without increasing the pressure in venous outflow(17).

PATHOPHYSIOLOGY:

Dural CCFs usually become symptomatic spontaneously. The pathogenesis of these fistulas is somewhat controversial. The pathogenesis of dural CCFs likely involves a primary thrombosis of cavernous sinus venous outflow channels and resultant vascular alterations to provide collateral flow. This theory of pathogenesis is widely supported because it also accounts for the development of arteriovenous fistulas involving other dural sinuses(15).

However, some authors favour a conflicting theory, which purports that dural CCFs form after the rupture of 1 or more of the thin-walled dural arteries that normally traverse the cavernous sinus(18). According to this hypothesis, after rupture, extensive preformed dural arterial anastomoses not directly involved in the fistula dilate and contribute collateral blood supply, resulting in an angiographic appearance indistinguishable from that of a congenital vascular malformation. Indeed, sequential arteriography demonstrates that the feeder vessels of dural CCFs change with time as the vessels spontaneously open and close(19). Although this theory is favored by some investigators(1), it fails to explain why spontaneous dural CCFs are more common in elderly women than in men.

Indirect CCFs tend to occur more frequently in postmenopausal women. The cause of these lesions is still obscure, but infants presenting with dural fistulas in the literature furnish some evidence to congenital origin(20). Factors that may predispose patients to the development of dural CCFs include hypertension, diabetes, pregnancy, trauma and straining, atherosclerotic disease, cavernous sinus thrombosis, sinusitis, and collagen vascular disease. Trauma is less commonly associated with indirect CCFs. Traumatic indirect CCFs differ from the spontaneous type because these lesions are usually single-hole fistulas in which the accessory meningeal artery and middle meningeal artery are found to be the most common feeders(21). Gao et al(22) suggested this may be due to loss of elasticity of the dural arterial wall with estrogen deficiency; whereas, Grove(23) proposed hormonal changes may promote coagulation and venous thrombosis with posterior venous drainage occlusion inducing symptomatology. There is support for the role of primary arterial fragility in CCF formation in the epidemiologic studies reporting spontaneous direct or indirect (dural) CCF development in patients with fibromuscular dysplasia, type IV Ehlers-Danlos, and osteogenesis imperfecta. There is also evidence for a hormonally induced hypercoaguable state given the increased incidence of CCFs in pregnancy(9).

CLINICAL FEATURES:

The cavernous sinus normally receives drainage from the superior and inferior ophthalmic veins as well as superiorly from the sphenoparietal sinus, sylvian veins, and cortical veins. The cavernous sinus drains posteriorly through the inferior petrosal sinus (IPS) and superior petrosal sinus to the jugular bulb, inferiorly through the pterygoid plexus *via* emissary veins, and contralaterally through the contralateral cavernous sinus(24).

A CCF allows highly pressurized arterial blood to be transmitted directly into the cavernous sinus and the draining veins, leading to venous hypertension. The clinical presentation of CCF is a direct consequence of elevation in intracavernous pressure and revised flow patterns. The revised venous drainage of the CCFs may head toward the ophthalmic venous system anteriorly; the superior petrosal sinus, the IPS, or the basilar plexus posteriorly; the sphenoparietal sinus laterally; the intercavernous sinus contralaterally; the pterygoid plexus *via* the vein of the foramen rotundum and the vein of the foramen ovale inferiorly. Most often, the direction of the venous drainage is multidirectional.

Presenting symptoms of CCFs may include a subjective bruit, diplopia, tearing, red eye, ocular foreign body sensation, blurred vision, and headache(25). Anteriorly draining fistulas are more likely to cause ocular symptoms(26). Patients with posteriorly draining fistulas may develop neurologic symptoms, such as confusion and expressive aphasia(27), as well as diplopia from isolated ocular motor nerve pareses. Clinical symptoms and signs usually are more indolent in dural fistulas. Clinical signs of CCFs depend in part on whether the lesion is high flow or low flow but include proptosis that may be pulsating in the setting of high flow lesions; a red-eye with arterialization of the conjunctival and episcleral vessels; chemosis; strabismus due to ocular motor nerve dysfunction, orbital congestion, or both; an ocular bruit; increased intraocular pressure

(IOP); stasis retinopathy or even central retinal vein occlusion in cases of significantly raised episcleral venous pressure; and optic neuropathy that may be non-glaucomatous from direct trauma or ischaemia, or glaucomatous. Although an objective bruit is more common in the setting of a high-flow fistula, it may be elicited with a Valsalva manoeuvre in some patients with low-flowfistulas. Neurogenic strabismus most commonly presents as a sixth nerve palsy. The relative frequency of sixth nerve involvement occurs due to the central location of the sixth nerve adjacent to the ICA within the cavernous sinus, placing it at higher risk of injury than the other cranial nerves that are located in the deep layer of the lateral wall of the sinus.

When dural CCFs drain posteriorly into the superior and inferior petrosal sinuses, they are usually asymptomatic. Dural fistulas that drain posteriorly sometimes cause brainstem congestion that may be associated with neurologic deficits(26). In addition, such fistulas rarely may produce intracranial Hemorrhage.

Suh et al. (28) divided 58 patients into four main symptom pattern

- Orbital pattern (chemosis, exophthalmos, pain, eyelid swelling): 53%
- Cavernous pattern (ptosis, diplopia, anisocoria, ophthalmoplegia): 71%
- Ocular pattern (decreased vision, IOC > 20 mm Hg ocular pain, glaucoma, retinal hemorrhage): 64%
- Cerebral pattern (seizures, hemorrhage): 5%

PREVALENCE OF CSDAVF:

Epidemiologic data regarding the overall incidence of both DAVFs as well as of DCCFs are limited. Because similar diagnostic and therapeutic measures apply to all dural fistulas, DCCFs and DAVF can be considered as one epidemiologic group of disease. For both, the association with menopause (54%) and puerperium (18%) and lower incidence in men is typical(29).

In a metaanalysis published by Awad et al. (30) in 1990, with an additional 17 cases, the incidence of AVFs in the CS among all DAVFs was 11.9%, whereas the relationship of "aggressive" to "non-aggressive" cases was 1:6.5. The true prevalence of DCCFs is difficult to assess because many patients present with mild symptoms, may undergo spontaneous resolution and are never diagnosed. According to series of several major endovascular centers, Type B–D DCCFs occur five times more frequently than Type A fistulas. Another difficulty in obtaining accurate numbers lies in the fact that many DCCFs patients are studied as different groups, either included in DAVFs, CCFs or evaluated as a separate entity. The series of Cognard et al. (31) contained 205 cases of DAVF of which 33 were DCCF (16%). Klisch et al.(32) reported on 17 CCFs, including 11 DCCFs. Satomi et al. 002) reported on 117 cases of benign DAVF (without cortical venous drainage) with DCCF representing the largest group (42.7%) (33). Tsai et al. investigated 69 patients with DAVFs among whom 30% involved the CS(34). Chung et al. found the CS as the most common (57%) location for the DAVF in 60 patients(35). Tomsick observed Type B–D fistulas in 68% of all spontaneous CCF(29).

NATURAL HISTORY OF DURAL CCFs

As true for prevalence and incidence of DCCFs, exact data on natural history do not exist, which is in part due to the fact that a large number of fistulas is discovered relatively late in their course. Furthermore, cases undergoing diagnostic angiography are necessarily affected by the angiographic procedure itself as contrast injection can accelerate thrombosis of the CS and "spontaneous occlusion"(29).

In some recent series (Satomi et al, Suh et al) the natural course is additionally influenced by particulate arterial embolization(28,33). The number of reported "spontaneous" occlusions reported in the literature may lie between 11% and 90% and is on average 35% according to Tomsick (29). Suh et al. have retrospectively studied the evolution of fistulas over a mean follow-up period of 23 months(28). They found that seven (30%) of their patients, angiographically classified as proliferative type (PT), showed chronological progression to the late restrictive type (LRT).

As for DAVFs, presence of leptomeningeal drainage is the main indicator for risk assessment and decision-making in patients with DCCFs by most authors. The number for cortical or leptomeningeal reflux varies from 10% to 31%. Nevertheless, the associated risk of intracranial hemorrhage (around 2%) seems, however, relatively low compared to patients with DAVFs in other locations, especially at the tentorial sinus or in the anterior cranial fossa. Consequently, cortical or leptomeningeal drainage in DCCFs must not necessarily be seen as an indicator of a progressive or "malignant" course or nature, as in DAVFs(29).

RADIOLOGICAL DIAGNOSIS OF DURAL CCF:

The clinical presentation of patients with characteristic neuro-ophthalmic symptoms does not usually require invasive imaging techniques, and a correct diagnosis can be made with certainty using CT or MRI techniques. If there is a clinical suspicion of an inflammatory or tumorous process in the orbital or peri-orbital region, computed tomography (CT) or magnetic resonance imaging (MRI) is commonly performed.

In the case of a CSDAVF, the image may show a dilated vein, indicating an underlying vascular pathology. Exophthalmos or a proptosis can often be diagnosed using a routine CT scan. However, only when the AV shunting volume is large enough will the CS become visible as an enhancing space-occupying lesion. A focal bulging or diffuse distension of the CS on contrast-enhanced CTs has been detected in 50%– 64% of the cases(36). The SOV can be enlarged on the fistula site in 86%–100% on post-contrast CTs and in 75%–100% on spin-echo MR images(37). If cortical venous drainage is present, those enlarged veins may become visible on axial CT. Watanabe et al. (1990) described a case of a Type D fistula with considerably enlarged veins visualized on contrast-enhanced CT(29).

Teng et al. (1991) reported a brain stem edema in two patients with Type D fistulas that became visible on CT after occlusion of the normal venous drainage, probably triggering the development of cortical venous drainage(21). In both cases, complete disappearance of the edema was documented(29). Uchini et al. (1997) reported two patients with pontine venous congestion due to CSDAVFs. Brain stem edema due to CSDAVFs has also been described by Takahashi et al(19,38,39) in two patients, in which after occlusion of the fistula, reversal of the edema on MRI became evident. Edematous changes due to venous hypertension can also be seen in both hemispheres being mainly limited to the white matter, like vasogenic edema.

MRI is superior to CT in showing discrete changes due to AV shunts of the CS, because it may demonstrate not only the enlarged SOV but also a minimal proptosis and extraocular thickening of the muscles. Sato et al. reported on flow voids shown in eight of 10 patients with Type D fistulas using spin echo sequences(33). MRA can be helpful in low-flow conditions, as often present in DCSFs. MRI findings can be discrete on MIPs and raw data (source images) can be useful for analysis(35).

MRA, as well as conventional spin echo sequences, can demonstrate abnormal cortical drainage (40). Several authors have described flow voids within the CS on spin echo MR images in patients with CSFs(37). Hirai et al saw flow voids in the CS less frequently in their patients and found in 3% false positive results, emphasizing the difficulty to differentiate normal venous flow in the CS from abnormal flow voids caused by an AV shunt based on spin echo MR images(41). The visualization of draining veins may require using both phase contrast techniques (3D PC MRA) for demonstrating the dilated SOV and associated reflux, and 3D TOF MRA for demonstrating the IPS. If the SOV is not the draining vein it may not be demonstrated with 3D PC MRA. The IPS is usually shown better on TOF MRA, because it runs in a superior inferior direction causing stronger time of flight effects(29). Hirai et al. have compared the value of fast imaging with steady state precession (FISP) to contrast enhanced CT and spin echo MR imaging and found it superior in the diagnosis of CCF(41). 3D FISP images showed posterior venous drainage, but were not helpful in detecting cortical drainage, which is an important detail not to be missed.

3D TOF MRA:

Because relying on MRI and 3D TOF MIP images alone may lead to underdiagnosis of indirect CSFs, MRA source images become quite valuable. Tsai YF et al. (2004) encountered dilemmas in reviewing MRI flow voids and identified them in only five of eight patients with DCSFs(42). The authors detected an engorged CS only in four cases and swollen extraocular muscles in none. Flow artifacts resulting from pulsation of the cavernous ICA may corrupt CS details and CSF pulsation may result in flow voids in the prepontine cistern mimicking enlarged abnormal vessels. Air in the sphenoid sinus may cause susceptibility artifacts or partial volume effects. Because MIP reconstruction may cause vascular distortion they need to be reviewed carefully. Reliance on MIPs alone may lead to misdiagnosis in 50% of the cases. On the other hand, reading of the source images of 3D-TOF MRA allowed the correct diagnosis in all eight cases. Therefore, in order not to overlook small AV shunts, careful evaluating of MRA source images should be included in all doubtful cases. Nevertheless, even with improved technology, MRI and MRA cannot replace high quality DSA for differentiating direct Type A and indirect Type D fistulas with certainty (Tsai YF et al. 2004)(34). Chen CC et al. (2005) have compared the utility of CTA and MRA source images in the diagnostic of 53 direct CCFs(40). They found CTA as useful as DSA and superior to MRA in accurately localizing the fistulous connection.

The diagnostic ability of unenhanced 3D TOF MRA at 1.5T for intracranial DAVFs is limited compared with that of DSA. Potential advantages of 3D TOF MRA at 3T compared to 1.5T include high signal-to-noise ratio (SNR) and prolonged T1-weighted relaxation times that improve contrast between vessel and tissue and acquisition of MRA images of high quality and high spatial resolution. Consequently, 3T 3D TOF MRA can be expected to provide precise information regarding the fistula site, arterial feeders, and venous drainage of DAVFs.In patients with DAVF, Azuma et al compared 3D non contrast TOF MRA at 3T with DSA in 26 patients. They got encouraging results of interobserver and intermodality agreement for fistula site, arterial feeder and venous drainage. (4).

Susceptibility-weighted angiography (SWAN):

Susceptibility-weighted angiography (SWAN) is a new 3D T2*- based gradient-echo sequence generating several echoes that are read out at different TE times.2 During each TR, the SWAN sequence captures multiple TE readouts: short TEs provide a time-of-flight (TOF) effect, whereas long TEs are responsible for the magnetic-susceptibility effect. Indeed, the SWAN sequence allows high-resolution visualization of both cerebral veins and arteries.

Studies comparing the role of SWI in CS DAVF are limited, and recently few studies have been reported the usefulness of this sequence in the evaluation of DAVF.

A study to determine the utility and accuracy of susceptibility-weighted MRI (SWI) for the detection of carotid cavernous fistulas showed that all cases and controls were reliably distinguished with SOV/SSS signal intensity ratio of 0.64 as cut-off. Direct CCF cases had consistently higher ratios than indirect CCF. SWI was highly sensitive for detection and differentiation of both direct and indirect CCF. Only one case of corticovenous reflux was missed by SWI. They concluded that SWI is useful for detection of CCF and to differentiate between direct and indirect CCF(43).

Nakagawa et al published a larger series of 17 patients with DAVF in 2013. They compared SWI with DSA in pre and post treatment evaluation of DAVF. They noted that pretreatment SWI images revealed hyperintensity within the cortical vein which was suggestive of presence of shunting with cortical venous drainage. This abnormal signal was noted to disappear in post treatment scans. They concluded that SWI could provide a good noninvasive option in evaluation and follow up of DAVF.(44)

In 2016 Hodel et al studied the combined accuracy of SWI and ASL in evaluation of intracranial shunting lesions. Out of their series of 63 cases, 10 were DAVF. This study showed an excellent correlation with DSA. They demonstrated that this combined use of ASL and SWI was a good non contrast option compared with CEMRA in evaluation of DAVF.(7)

Jain et al in their series of 26 patients assessed the role of SWI in pretreatment evaluation of patients with intracranial DAVF. They specifically evaluated localization of fistula, cortical venous reflux and venous ectasia. Their study showed a significant difference between SWI and conventional MRI sequences with high accuracy rates for SWI. They suggested inclusion of SWI in routine pretreatment imaging of DAVF.(5)

SILENT MRA:

Silent MRA is a novel angiographic technique is a distinctive novel sequence, primarily for its almost none to minimal noise generation on being endowed with algorithm for Silent scan technique by GE healthcare and also for its excellent vascular depiction cum background suppression in virtue of being an ASL based subtraction technique incorporating an ultrashort TE(20–22). In this sequence, the vascular tree is explored by subtraction between a control image and a labelled image acquired after a cervical level labelling pulse. The Ultrashort TE also aids in minimizing the phase dispersion of the labelled blood and likewise decreasing the susceptibility effects.

Prior studies have(8) evaluated for ASL based Silent MRA technique mostly in comparison with the other prominent TOF angiographic imaging – TOF MRA. Kokzoglu et al evaluated 3D ASL MRA in assessment of Carotid stenosis using carotid vascular phantom which revealed its superiority 3D TOF in hemodynamically significant carotid stenosis(45).

In studies by Irie at al(46) and Takano et al(47) the Silent MRA technique was assessed in follow up of aneurysms post stent assisted coiling. Both authors were able to demonstrate the robustness of Silent MRA over TOF. Some of few anecdotal reports on the utility in AVM in vascular lesions and AVM were available from Suzuki et al(48) and in a case report by Jin II Moon et al (8). However, there are no case reports or studies on utility of the Silent MRA in CSDAVFs.

ORBITAL DOPPLER:

Color Doppler imaging can assist in diagnosis and follow-up of patients with CCFs. The findings of dilated SOV (diameter >2 mm), with reversed, arterialized, low-resistance blood flow (RI < 0.5), was considered diagnostic for the presence of a CCF with anterior drainage. Ophthalmic artery, also characterized by a flow directed toward the globe, but with an higher resistive index usually more than 0.7. Ophthalmic artery has a more curvilinear course than a dilated SOV with arterialized blood flow(29).

DIGITAL SUBTRACTION ANGIOGRAPHY:

DSA is universally accepted as the gold standard modality in evaluation of intracranial CSDAVF. It has unmatched temporal resolution, spatial resolution and contrast resolution and is presently the investigation of choice for confirmatory diagnosis and also for post treatment follow up of CSDAVF patients. DSA information is also central and essential for planning any neurointerventional procedure.

A complete DSA study should include a 6-vessel angiography including bilateral ICAs, ECAs and vertebral arteries. Selective injections of ECA branches and 3D rotational angiogram from the main involved feeding artery is essential in accurate diagnosis and treatment planning.

The arteriogram should provide the following angiomorphological information:

- Localization of the fistula site
- Differentiation between indirect and direct fistula
- Demonstration of the entire arterial supply, in particular in cases with DCCF with visualization of so-called “dangerous anastomoses”
- Visualization of the CS and its tributaries with possible stenosis, thrombosis, ectasias, draining veins such as IPS, SOV, ICS etc.
- Identification of CS varices, intercavernous pseudoaneurysms or cortical drainage

The aim of angiography in patients with dural CCF is to determine the exact location of the arteriovenous communication, and to decide which compartment of the CS is involved: anterior or posterior (or both), left or right. Dural arteries can cross the midline to supply an AV shunt at the contralateral CS, occasionally even when there is no significant ipsilateral supply.

Lasjaunias et al. have recommended performing selective catheterizations using even a microcatheter if necessary, to visualize the smallest pedicles and to identify the so-called “dangerous anastomoses” (49). Being aware of their existence is indispensable for avoiding ischemic complications during transarterial embolizations in ECA branches.

Use of 3D rotational angiography, permits identification of the fistula point and downstream venous sac. This detailed anatomic characterization of the fistula may improve treatment planning in the future. For successful embolization of the CSDAVFs, it is important to know the location of the shunted pouch. Previous reports by Kiyouse et al, showed that most fistulous points of CSDAVFs were detected in the posterior portion of the cavernous sinus, selective embolization of the shunted pouch or a compartment of the cavernous sinus is advantageous in that it allows the reduction of shunt flow using a small number of coils without increasing the pressure in venous outflow(17).

In 2017, Kannath et al localized CSDAVFs with the help of 3D rotational angiography and correlated the observations with clinical and angiographic findings. CSDAVFs were categorized as dural, extradural or osseous based on the site of convergence of feeders into the venous sac. Extradural CSDAVFs were further subcategorized into posteromedial, posterolateral and anterior subtypes, depending on proximity to a possible venous plexus. This classification was correlated with various clinical presentations and angiographic subtypes. The sac was identified in all the patients and the mean sac size of the fistula was small (< 4 mm). Dural type was associated with exclusive cortical venous drainage. Extradural anterior CSDAVF showed tendency towards younger age predilection. Extradural posterolateral CSDAVF was more often associated with initial oculomotor nerve palsy and this observation was statistically significant. Discordancy between the location of the fistula and the side of clinical affection was observed in midline fistulas such as osseous CSDAVF and posteromedial type of extradural CSDAVF(50).

Even though DSA remains the gold standard and the only validated modality to provide all the relevant details required for therapeutic decision making, it is not without its own demerits in the form of procedural complications and adverse contrast reactions not mentioning radiation hazard of repeated studies. Kaufman et al in their large series have reported a neurological complication rate of approximately 2% and mortality rate of 0.06% with diagnostic angiographic procedures(2).

TREATMENT:

Treatment options for dural CCFs include observation, IOP -lowering agents, intermittent compression of the ipsilateral ICA or SOV, stereotactic radiosurgery, and endovascular intervention.

CONSERVATIVE MANAGEMENT:

As up to 70% of dural CCFs close spontaneously due to local thrombosis of the SOV propagating posteriorly, observation or conservative treatment techniques not only are acceptable but also are the preferred approaches to management in cases without high-risk features(51). Initially, spontaneous closure may be associated with exacerbation of the clinical symptoms and signs; in this setting, patients may require repeat angiography. Closure of dural CCFs also has been reported after diagnostic angiography and air travel. If invasive intervention is not warranted, patients may use techniques of occlusion, such as external manual carotid compression, to promote resolution of the CCF(52). After exclusion of patients deemed to be poor candidates for carotid compression therapy, due to decreased visual acuity or cortical venous drainage of the fistula, success rate of this procedure has been reported to be 35%, with resolution occurring between 2 weeks and 7 months after initiation. Although a watchful waiting approach is reasonable in many patients with a dural CCF, treatment sometimes is required to prevent long-term sequelae. Indications for intervention include uncontrollable IOP, unremitting diplopia, severe proptosis with corneal exposure, optic neuropathy, retinal ischemia, severe bruit, and cortical venous drainage from the fistula.

ENDOVASCULAR TREATMENT:

The goal of treatment is to interrupt fistulous communications and decrease pressure in the cavernous sinus. This can be accomplished by occludng the arterial branches supplying the fistula (trans arterial embolization) or, more commonly, by occluding the cavernous sinus that harbors the fistulous communications (transvenous embolization) (53)

TRANSARTERIAL APPROACH:

Transarterial embolization of indirect low-flow CCFs generally is cumbersome because of the small size, complex anatomy, and multiplicity of arterial feeders. Additionally, potential complications (e.g., thromboembolic stroke, cranial nerve palsies) restrain the choice of the transarterial approach as the mainstay treatment of spontaneous indirect CCFs. Therefore, transarterial embolization is typically used only to reduce arterial inflow before transvenous occlusion for highflow indirect CCFs and as a viable alternative after failure of transvenous attempts.(54)

TRANSVENOUS APPROACH:

A transvenous approach via the IPS, is preferred for most dural CCFs that require treatment(55). The IPS is the first-line approach, as it is the most straightforward and shortest route to the cavernous sinus. Advances in endovascular technology, including the development of variable stiffness microcatheters and guidewires, have increased feasibility of this approach such that it is now possible in most patients. To access the IPS, a posterior approach via the internal jugular vein is used. When the IPS approach is not possible due to anatomic venular variations or thrombosis, an SOV approach may be used(56).

The SOV is approached via facial vein or other approaches like an anterior orbitotomy, and a venous catheter is then advanced through the SOV into the cavernous sinus. Although most patients with a CCF have dilation of the SOV, an SOV that is fragile, small, thrombosed, or associated with other vascular anomalies (eg, varices) may elude cannulation. Nonetheless, success of this approach has been reported even in the setting of SOV thrombosis.

A recent systematic review reported a 90% success rate with no major complications among CCF embolization procedures completed via an orbital approach. Coils commonly are used in transvenous procedures.

The success rate for transvenous procedures is ~ 80%, albeit with a centre-dependent complication rate that ranges up to 20%. Reported complications include ocular motor nerve palsies; trigeminal sensory neuropathy; brainstem infarction; significant IOP elevation; intracranial haemorrhage; pulmonary emboli; and orbital haemorrhage in the setting of the SOV or inferior ophthalmic vein approach. Although the risk involved necessitates careful patient selection, successful endovascular treatment can lead to marked improvement in signs and symptoms.(56)

STEREOTACTIC RADIOSURGERY (SRS):

When an endovascular approach is not feasible or has been unsuccessful, stereotactic radiosurgery (SRS) may be considered for treatment of a dural CCF. Using a therapeutic radiation dose of 20–50 Gy, SRS induces an injury of the targeted vessel, thus obliterating the vessel lumen. It has the benefit of being less invasive than endovascular embolization, although the treatment effect is delayed by several months, which makes the procedure inappropriate for patients at risk for acute visual or neurological decompensation. Reports of complete resolution of a CCF with SRS treatment range from 50 to 100%. The risk of immediate complications is low; however, data on late radiation-induced complications are limited.(57)

Most CSDAVFs can be diagnosed clinically. Invasive treatment usually is not required in most cases of low-flow fistulas, as these may close spontaneously. For patients with high-flow fistulas and those in which there is cortical venous drainage, successful closure usually can be achieved with an acceptably low morbidity and virtually no mortality using current endovascular techniques.

To our knowledge, there are no systematic studies on the reliability of unenhanced 3T 3D TOF MRA, Silent MRA and SWAN for assessing feeders, fistula sites, and venous drainage of CSDAVFs. Thus, this intended to study the utility of these noninvasive magnetic resonance angiography techniques to determine the angiomorphology of CCF, in treatment planning and follow up.

MATERIALS AND METHODS:

This was a prospective study conducted after obtaining the institutional ethics committee approval from October 2017 to June 2019. Informed written consent was obtained from all the participants who were part of this study.

Consecutive patients with CSDAVF, presenting to the SCTIMST interventional radiology, neurosurgery, neurology clinics and by direct referrals and consultations from other departments were considered for inclusion. These patients underwent magnetic resonance imaging as per the below-stated protocol. Digital subtraction angiography was also done as per standard guidelines followed in the institution. Magnetic resonance imaging and Digital subtraction angiography were obtained within a gap of 2 weeks. The 3D TOF MRA image datasets, Silent MRA data sets, SWAN data sets, DSA images, and three-dimensional rotational angiogram image sets were analyzed separately. The images sets were read with a time gap of at least 2 weeks to exclude memory bias. The 3D-TOF, Silent MRA, SWAN, and the Digital subtraction angiography, were analyzed for the image quality and graded on a 4-point scale. Then the 3D-TOF, Silence MRA, SWAN, and the DSA were evaluated independently for following parameters: the location of the Carotid-Cavernous Fistula, laterality, size of fistula, feeding arteries venous drainage and cortical reflux. After collection of data statistical analysis was done to generate the inferences

Inclusion criteria:

• All consecutive patients with indirect CCF presenting to SCTIMST neurosurgery, neurology or radiology clinics

• Patients who needed Digital subtraction angiography to assess completion of treatment.

• Patients who were not evaluated with magnetic resonance angiogram or Computed tomography angiogram at SCTIMST/elsewhere

• Patients whose angiographic images were suboptimal or of poor interpretable quality and needed further imaging studies at SCTIMST.

Exclusion criteria

• Patient or relatives declining consent

• Claustrophobic patients, patients with 3Tesla incompatible metallic implants, pacemakers or cochlear implants.

• Contraindication for iodinated contrast (DSA).

• Brain vascular lesions other than indirect Carotid-Cavernous Fistula.

STUDY PROTOCOLS AND PARAMETERS – MRI AND DSA:

Consecutive patients with indirect Carotid-Cavernous Fistula were considered for inclusion. These patients underwent Digital subtraction angiography and Magnetic resonance imaging as per the stated protocol. The Digital subtraction angiography was done in Interventional Radiology Suite at SCTIMST on General Electric Innova biplane 3131 and Magnetic resonance imaging was done on General Electric Discovery 750E 3.0 Tesla machine. The MRI protocol for the Study included the following sequences, 1. 3DTOF MR angiogram (TR/TE, 19/2.9 msec; flip angle, 15°; field of view, 200×200 mm; matrix, 416×192; section thickness, 1.2 mm; NEX, 1; bandwidth, ±41.7 kHz; acquisition time, 3 min 31 s.) 2. Silence MR angiogram (TR/TE, 1116.4/0.016 msec; flip angle, 5°; field of view, 180×180 mm; matrix, 150×150; section thickness, 1.2 mm; number of excitations (NEX), 1.5; bandwidth, ±20 kHz; acquisition time, 7 min 40 s.) 3. SWAN angiogram (TR/TE, 42/28 msec; flip angle, 15°; field of view, 220×220 mm; matrix, 288×384; section thickness, 2.4 mm; NEX, 1; bandwidth, ±31.2 kHz; acquisition time, 4 min 5 s). The MRI and Digital subtraction angiography images were obtained from PACS, anonymized and stored separately in numbered folders. The anonymized images in the separate folders were analyzed independently.

Statistical analysis of the data was performed using the Statistical Package for Social Science Version 23. Cohen's kappa coefficient statistical parameters were used to look for agreement between the two methods. Wilcoxon signed-rank test was used for assessment of the difference in assigned diagnostic scores. The ability of depiction of quantifiable characteristics was statistically evaluated by using logistic regression (chi-square test) to test the significance of differences between 3D-TOF, Silence MRA, SWAN and with DSA. Statistical significance was assessed using the p-value < 0.05.

OBSERVATION AND RESULTS:

DEMOGRAPHICS:

The study included a total of 37 consecutive patients (6 males and 31 females; age range 45 - 80 years; mean [SD] 59.5 ± 9.5 years). 67 % (25 patients) of the cases were in the age group of 50 to 70 years. There were 16 (43%) cases with the right, 18 (49%) cases with left and three (8%) cases with bilateral CCF.

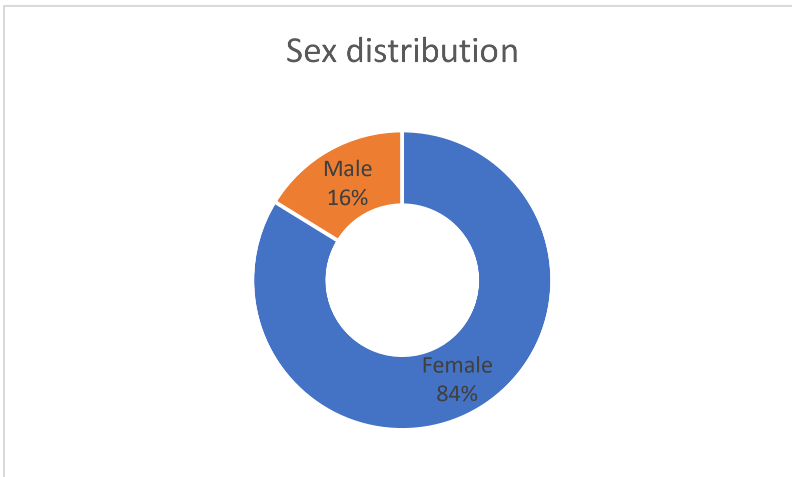

Figure 1. Sex distribution.

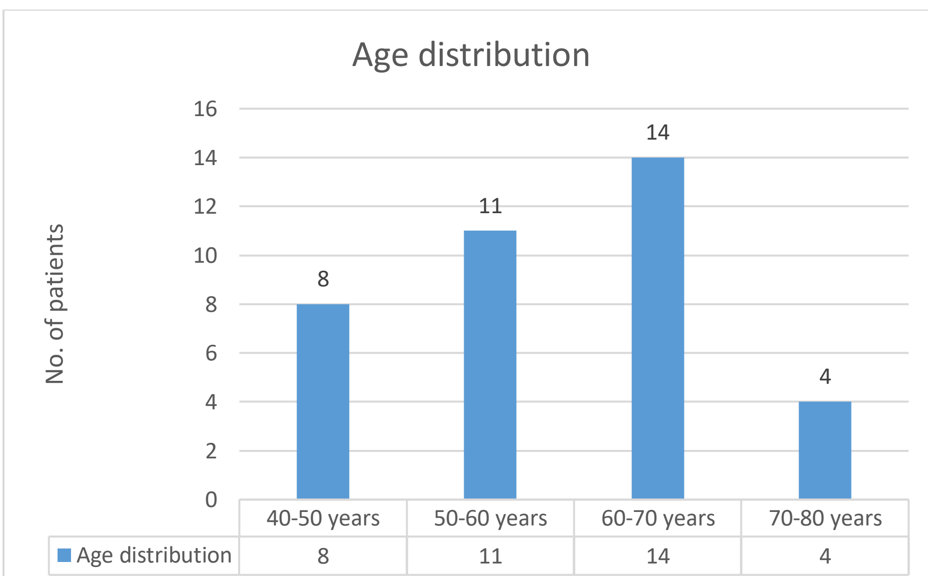

Figure 2. Age distribution

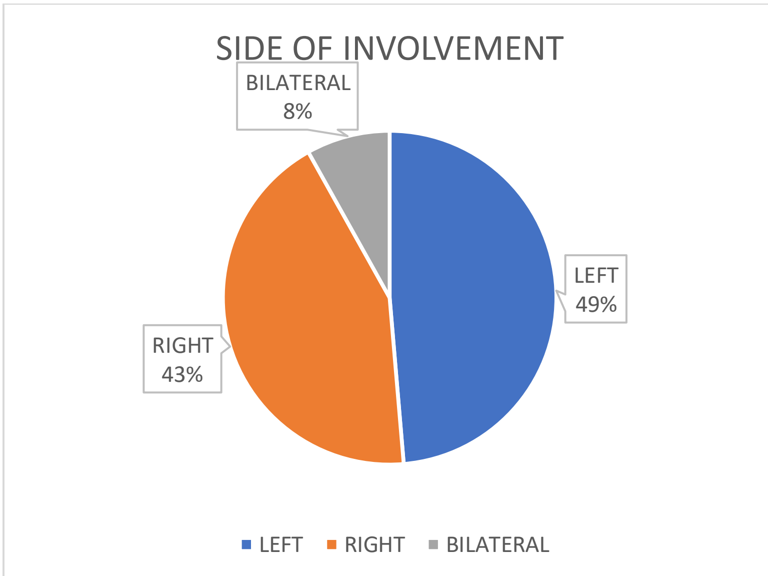

Figure 3. Side of involvement

CLINICAL FEATURES:

Most patients presented with orbital symptom pattern (86.4 %). Cranial nerve palsies (Cavernous symptoms) were noted in 75% of patients. The specific symptoms and signs are presented in Figure 4. The most prevalent sign was proptosis and the least prevalent was seizures, which was seen in one patient.

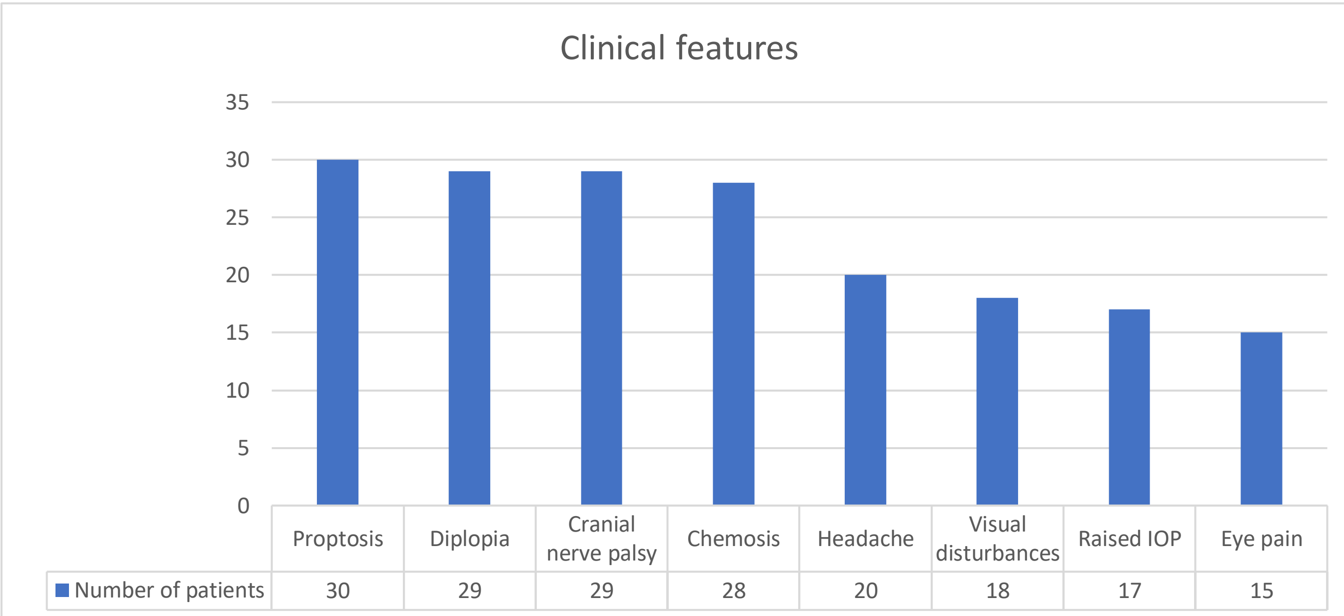

Figure 4: Clinical features.

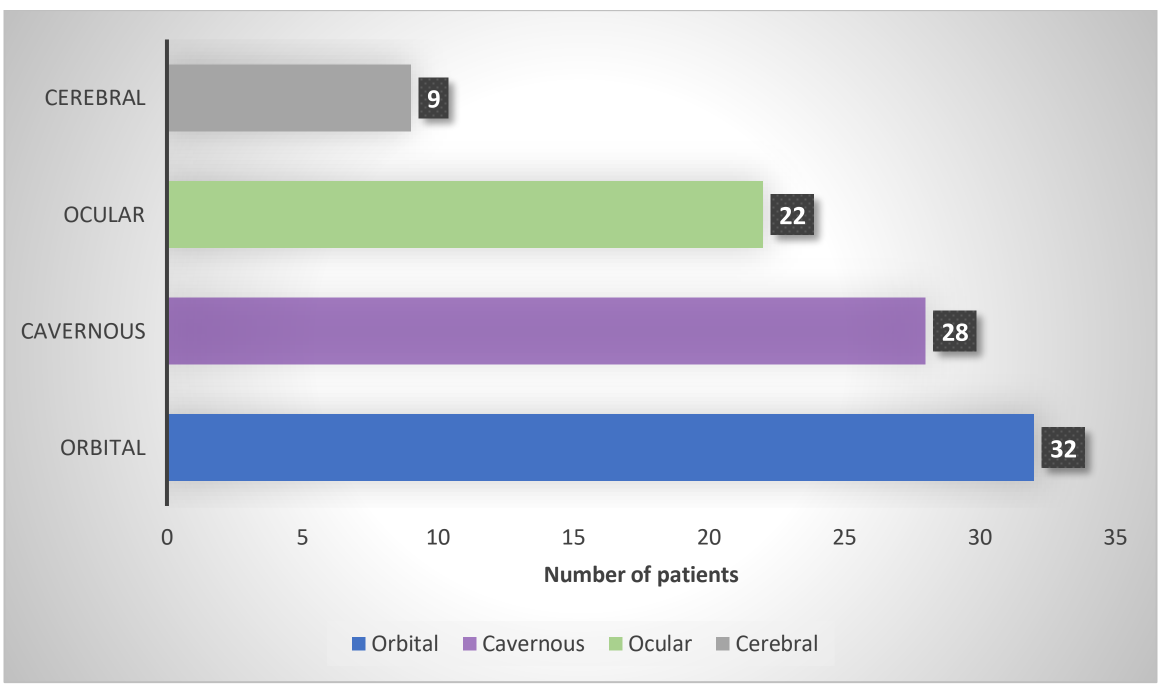

Figure 5: Symptom Pattern

ANGIOARCHITECUTRE:

Barrow's Type:

34 of the 37 patients were of Barrows Type D, 2 were of Type C and 1 of Type B. 31 patients had bilateral supply and 6 patients had unilateral supply.

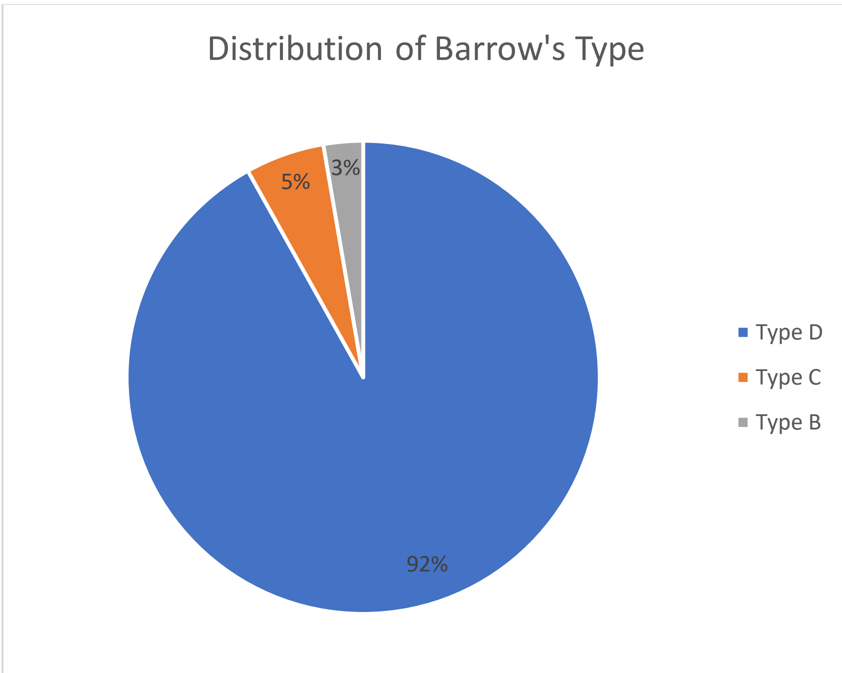

Figure 6: Distribution of Barrow's Type.

Location of fistula:

Most common site of fistula being the postero medial location (45%), followed by postero lateral location (26%), anterior (16%) and midline or intercavernous sinus location (13%). In four patients site of the fistula could not be made out clearly.

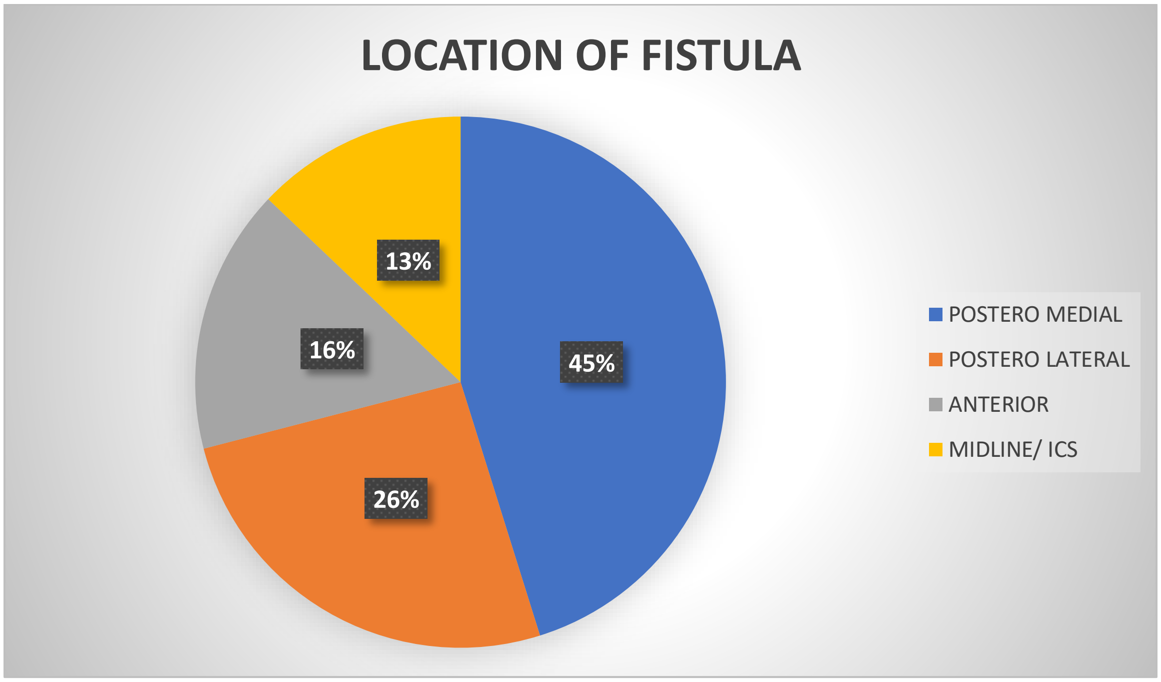

Figure 7: Location of Fistula

SUH ANGIOGRPAHIC TYPE:

CSDAVF presents as 3 distinctive angiographic types. 15 patients had proliferative pattern, 13 had restrictive pattern and 9 had late restrictive pattern.

Gender Difference According to the Angiographic Type of CSDAVF

Type	Male	Female	No. of Patients
Proliferative	0	15	15
Restrictive	3	10	13
Late restrictive	3	6	9
Total (%)	6 (17)	31 (83)	37 (100)

Table 1: Gender Difference According to the Angiographic Type of CSDAVF

PT (n=15) and RT (n=13) of CSDAVF were more common than LRT (n=9).

The differences in the presenting symptom patterns were related to the venous drainage patterns. CavSxP was related to the posterior venous drainage (*P*=0.041) and CerSxP to the SMCV drainage (P=0.001) and cortical venous reflux (P= 0.004).

Difference in Presenting Symptom Patterns According to the Angiographic Types of CSDAVF

Presenting Type	Orbital Pattern	Cavernous Pattern	Ocular Pattern	Cerebral Pattern	No. of Patients
Proliferative	12	11	9	5	15
Restrictive	11	10	5	1	13
Late restrictive	9	7	8	3	9
Total (%)	32(86)	28(75)	22 (59)	9 (24)	37 (100)

Table 2: Difference in presenting symptom patterns according to the angiographic types.

Relation of Angiographic Types and Venous Drainage Pattern:

The difference in the venous drainage was also related to the angiographic type. Absence of IPS venous drainage and presence of deep venous drainage is significantly associated with late restrictive type.

Type of Venous drainage		Proliferative		Early restrictive		Late restrictive		χ^2	p
		Count	Percent	Count	Percent	Count	Percent		
IPS DRAINAGE	Absent	5	33.3	10	76.9	9	100.0	12.25**	0.002
	Present	10	66.7	3	23.1	0	0.0		
DEEP VENOUS DRAINAGE	Absent	5	33.3	6	46.2	9	100.0	10.57**	0.005
	Present	10	66.7	7	53.8	0	0.0		

**: - Significant at 0.01 level, *: - Significant at 0.05 level

Table 3: Venous drainage pattern according to the presenting types

Venous drainage and CVR:

Anterior drainage into SOV was seen in 32 patients (86%). Only SOV drainage was seen in 6 patients. Superior drainage into SMCV was seen totally in 19 patients (51%). IPS drainage was seen in 13 cases (35%).

Cortical venous reflux into cortical veins through SMCV, Basal vein of Rosenthal and perimesencephalic veins were seen in 22 patients (59%).

Deep venous and pontomedullary venous reflux were seen in 17 patients, with primary venous connection through superior petrosal sinus in 8 patients, and through uncal and bridging veins in rest of the patients.

VENOUS DRAINAGE	NO. OF PATIENTS	PERCENTAGE (%)
ANTERIOR -SOV	32	86
SUPERIOR - SMCV	19	51
INFERIOR – IPS	13	35
POSTERIOR -SPS	10	27
CVR – SMCV/ BVR	22	59
DEEP VENOUS DRAINAGE-BVR OR BRAINSTEM VEINS	17	46

Table 4: Venous drainage pattern and CVR.

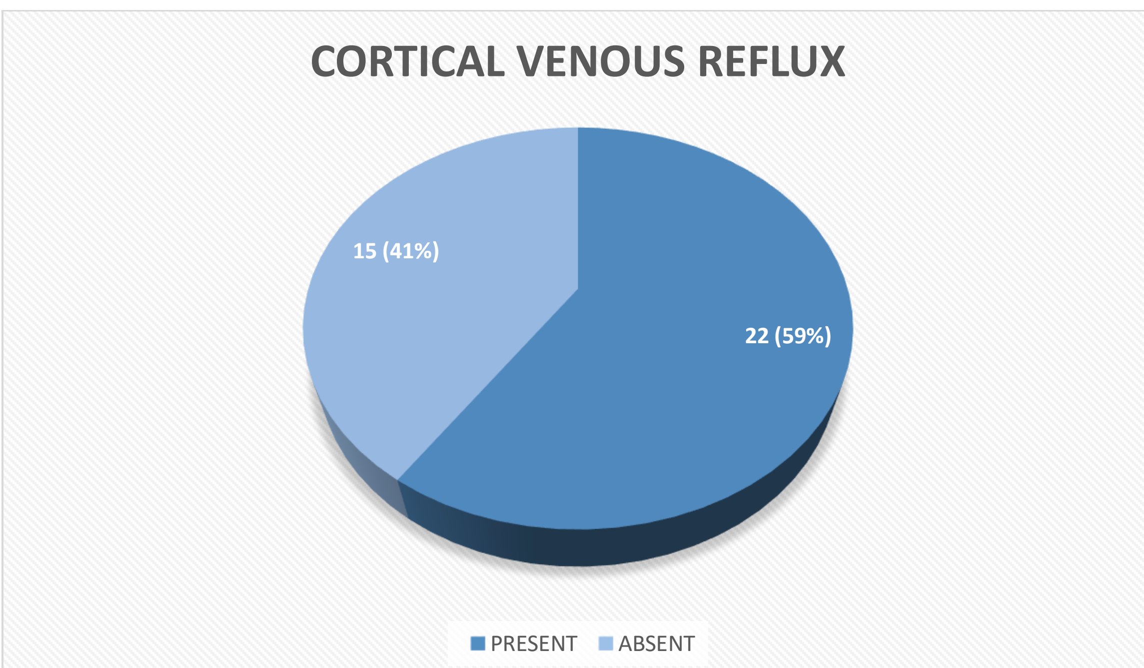

Figure 8: Cortical venous reflux

Arterial feeder characterization and detection:

There were totally 210 arterial feeders identified in 37 patients in this study. Most common arterial feeders are from distal branches of the IMA (internal maxillary artery) and cavernous branches of the ICA (MHT or ILT). Bilateral arterial feeders are noted in 31(84%) patients and unilateral feeders are noted only in 6 (16%) patients.

TOF MRA correctly identified 188 (89.5%) of the 210 arteries which were feeding the fistula and confirmed on DSA. Silent MRA correctly identified 195 (92.8%) of the 210 arterial feeders. The percentage of feeding arteries which were missed on Silent MRA and TOF were 7.2% for Silent MRA (15 feeders) and 10.5 % (22 feeders) for TOF MRA. The intermodality correlation between TOF and DSA was moderate, with kappa value of 0.595 ($p<0.0001$). The intermodality correlation between Silent and DSA was substantial, with kappa value of 0.719 ($p<0.0001$).

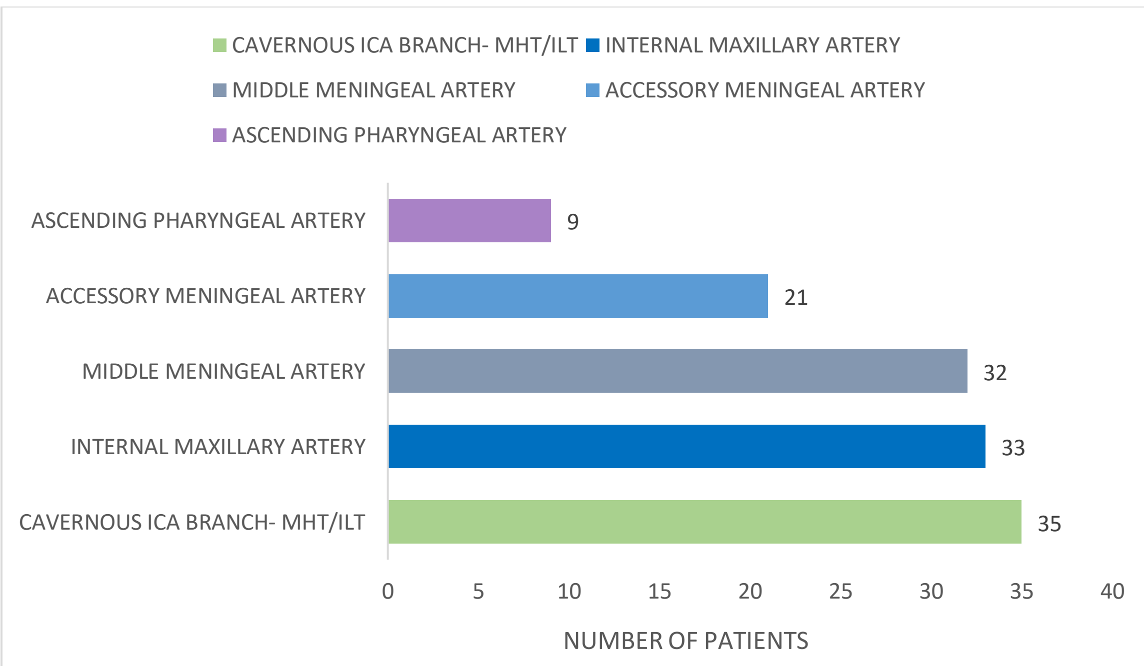

Figure 9: Types of Arterial feeders

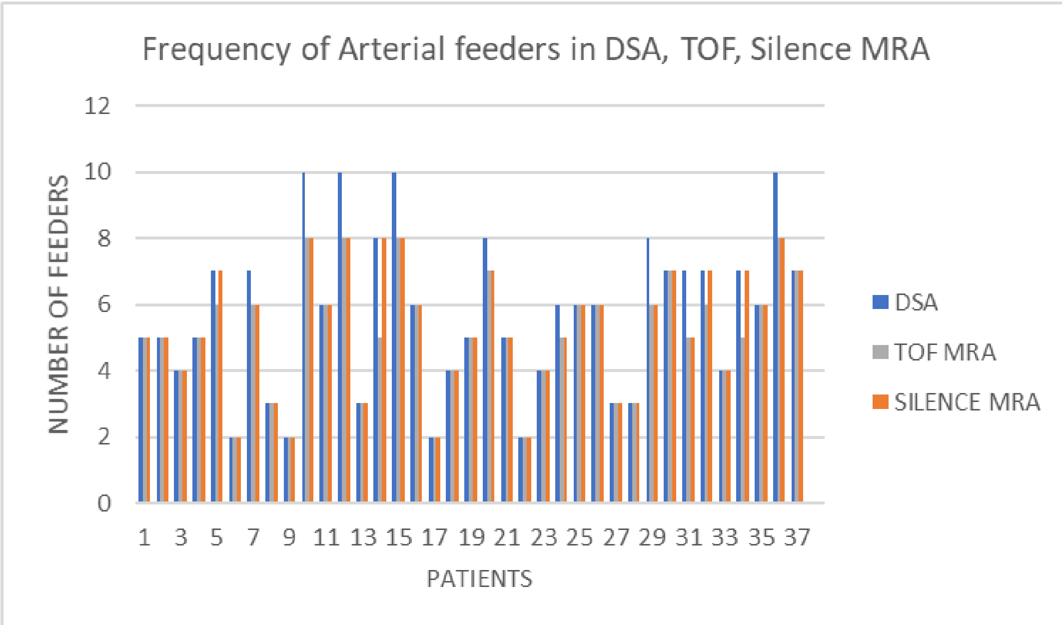

Figure 10: Frequency distribution of arterial feeders on DSA, TOF MRA and Silent MRA.

VENOUS IDENTIFICATION:

Totally 74 draining venous channels were identified on DSA in the 37 cases of CSDAVF assessed in this study. Of these 90 % were correctly identified on Silent MRA as to 85% identified on TOF. The intermodality correlation between TOF MRA and DSA was moderate, with kappa value of 0.403 ($p<0.0001$). The intermodality correlation between Silent MRA and DSA was substantial, with kappa value of 0.648 ($p<0.0001$).

VENOUS IDENTIFICATION	SILENT MRA	TOF MRA	SWAN
CORRECT	67 (90%)	63 (85%)	53 (71%)
MISSED	7(9.4%)	11 (14.8%)	21 (28.3%)
MISINTERPRETED	1 (1.3%)	3 (4%)	2 (2.7%)

Table No: 5–Comparison of Venous Visualization On Silent And TOF MRA

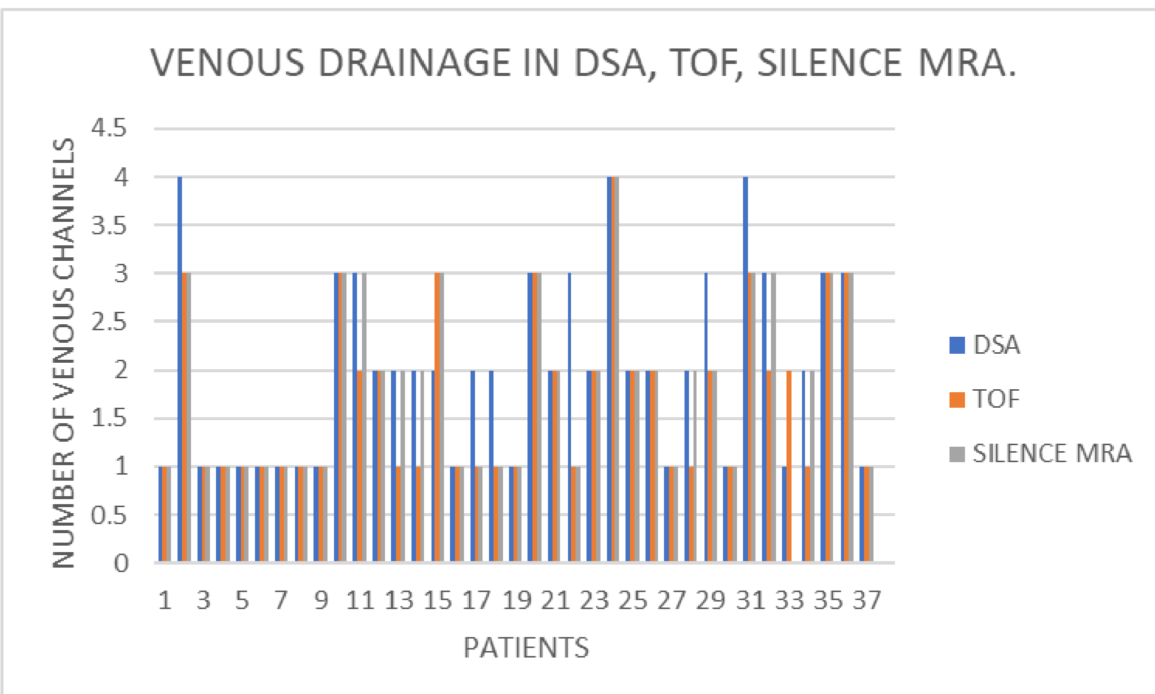

Figure 11: Frequency distribution of venous drainage in DSA, TOF and Silent MRA.

VENOUS DRAINAGE DETECTION:

ANTERIOR VENOUS DRAINAGE- SOV:

Silent MRA had a sensitivity of 93.8 %, specificity of 100%, PPV of 100% and NPV of 71.4% for the detection of anterior venous drainage. TOF MRA reported a sensitivity of 84.4%, specificity of 100%, PPV of 100 % and NPV of 50% for anterior venous drainage detection. SWAN reported a sensitivity of 87.5%, with a specificity of 80%.

POSTERIOR DRAINAGE – SPS:

Silent MRA and TOF MRA both had a sensitivity of 60 %, specificity of 100%, PPV of 100% and NPV of 87.1% for the detection of SPS venous drainage. SWAN reported a sensitivity of 20 %, specificity of 100%.

INFERIOR VENOUS DRAINAGE- IPS:

Silent MRA had a sensitivity of 84.6 %, specificity of 95.8%, PPV of 91.7% and NPV of 92% for the detection of IPS venous drainage. TOF MRA reported a sensitivity of 69.2%, specificity of 95.8 %, PPV of 90 % and NPV of 85.2 %. SWAN reported a sensitivity of 46.2%, with a specificity of 100%.

SUPERIOR VENOUS DRAINAGE- SMCV:

Silent MRA had a sensitivity of 94.7 %, specificity of 100%, PPV of 100% and NPV of 94.7 % for the detection of SMCV drainage. TOF MRA reported a sensitivity of 84.2%, specificity of 88.9 %, PPV of 88.9 % and NPV of 84.2 %. SWAN reported a sensitivity of 89.5%, with a specificity of 88.9%.

VENOUS DRAINAGE	MODALITY	SENSITIVITY	SPECIFICITY	PPV	NPV	ACCURACY	KAPPA
SOV	SILENT	93.8	100	100	71.4	94.6	0.8
	TOF	84.4	100	100	50	86.5	0.59
	SWAN	87.5	80	-	-	-	0.52
SPS	SILENT	60	100	100	87.1	89.2	0.69
	TOF	60	100	100	87.1	89.2	0.69
	SWAN	20	100	-	-	-	0.26
IPS	SILENT	84.6	95.8	91.7	92	91.9	0.82
	TOF	69.2	95.8	90	85.2	86.5	0.69
	SWAN	46.2	100	-	-	-	0.52
SMCV	SILENT	94.7	100	100	94.7	97.3	0.95
	TOF	84.2	88.9	88.9	84.2	86.5	0.73
	SWAN	89.5	88.9	-	-	-	0.78
DEEP VENOUS DRAINAGE	SILENT	82.4	95	93.3	86.4	89.2	0.78
	TOF	64.7	95	91.7	76	81.1	0.61
	SWAN	58.8	100	-	-	-	0.60
CVR	SILENT	90.9	100	100	88.2	94.6	0.89
	TOF	81.8	93.3	94.7	77.8	86.5	0.73
	SWAN	86.4	93.3	-	-	-	0.78

Table No: 6–Comparison of Sensitivity, specificity, PPV, NPV and Accuracy for venous drainage on Silent, TOF, SWAN vs DSA.

INTERMODALITY CORRELATION:

LOCATION OF THE FISTULA:

In the detection of the site of fistula, the TOF MRA was concordant with DSA in 75 % (28) of the cases (Kappa =0.66; p<0.001). The discordance was more with the detection of the location in the midline or intercavenrous sinus, which was mistaken for posteromedial CS in 3 cases. Silent MRA was concordant with DSA in 32 cases (86%), with a Kappa value of 0.82; p<0.01.

SUH ANGIOGRAPHIC TYPE:

In the identification of the SUH type, the TOF MRA was concordant with DSA in 75 % (28) of the cases (Kappa =0.66; p<0.001). The discordance was more with the restrictive and late restrictive pattern. Silent MRA was concordant with DSA in 31 cases (83%), with a Kappa value of 0.75; p<0.01.

ANGIOGRAPHIC PARAMETER	TOF	SILENT
Location of fistula	28(75%) k =0.66	32(86%) k= 0.82
SUH type	28 (75%) k=0.63	31(83%) k=0.75

Table 7: Agreement between TOF vs DSA and for Silent MRA vs DSA.

SWAN FINDINGS:

Microbleeds were noted in 9 cases out of 37 patients in this study. Microbleeds were commonly seen in the temporal lobes, followed by fronto-parietal lobes and cerebellum. Two patients had pontine hyperintensities in the FLAIR sequence suggesting ischemia/ venous congestion. Microbleeds and venous congestion were significantly related to presence of SMCV venous drainage (P<0.01) and Cortical venous reflux (P=0.002).

Type of Venous Drainage		Brain finding				χ^2	p
		No		Yes			
		Count	Percent	Count	Percent		
SMCV	Absent	18	100.0	0	0.0	12.98	p<0.01
	Present	9	47.4	10	52.6		
CVR	Absent	15	100.0	0	0.0	9.34	p=0.002
	Present	12	54.5	10	45.5		

Table 8: Relationship between MRI Brain parenchymal findings and Venous drainage.

SOV/SSS SIGNAL INTENSITY:

Mean ± Standard deviation of SOV/SSS signal intensity ratios for group 1(indirect CCF cases), group 2 (controls- non vascular pathology) were 0.87 ± 0.96 and 0.43 ± 0.52 respectively. Student t test (two-tailed) between group 1 and 2 for detecting CCF was statistically significant with p<0.0001.

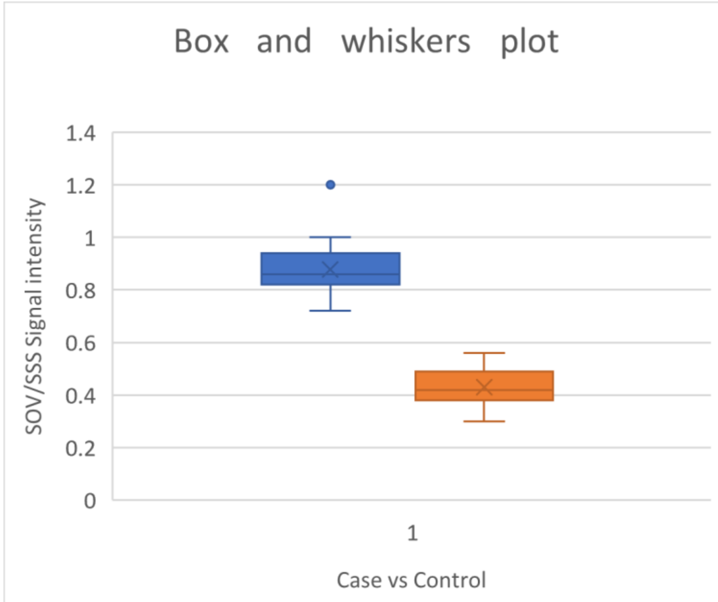

Figure 12: Box and Whiskers plot for SOV/SSS signal intensity.

EVALUATION OF DIAGNOSTIC CONFIDENCE SCORES ACROSS MODALITIES

The DC scores were assessed for the CSDAVF characteristic including arterial feeders, fistula and venous drainage. The diagnostic confidence was graded as per a 4-point Likert scale which was defined as, Grade 1- non diagnostic images, 2 – faint visualisation and difficulty in diagnosis. 3 – moderate visualisation with some blurring due to artefacts but diagnostic, 4 good quality images with definite diagnosis possible.

The difference in DC scores between Silent vs DSA and TOF MRA vs DSA was computed. Assuming the null hypothesis to be true with no statistically significant imaging quality difference between the modalities, the difference expected would be zero. The non-parametric paired t test, Wilcoxon signed rank test, was used to determine if a statistically significant difference in image quality was present between the two modalities assessed. Statistical significance was assumed with a P value of <0.05.

	MODALITY	ARTERIAL FEEDER VISUALISATION	FISTULA	VENOUS DRAINAGE
MEAN OF DC SCORES	SILENT MRA	3.89	3.54	3.78
	TOF MRA	3.83	2.96	3.21
	DSA	3.97	3.90	3.97
Wilcoxon signed rank test, p value comparing difference in DC between DSA with Silent MRA and DSA with TOF MRA		0.150	<0.01	<0.01
Mean of difference in DC between DSA and Silent MRA		0.08	0.36	0.19
Mean of difference in DC between DSA and TOF MRA		0.14	0.94	0.76

Table No: 9–comparison of diagnostic confidence scores across modalities for various CS DAVF characteristics.

The mean of the Diagnostic confidence scores for feeding arterial detection was 3.89 for Silent, 3.83 for TOF MRA and 3.97 for DSA. The DC score for fistula identification was 3.54 for Silent MRA, 2.96 for TOF MRA and 3.90 for DSA. For venous drainage, the same was 3.78 for Silent MRA, 3.21 for TOF MRA and 3.97 for DSA.

Wilcoxon signed rank test was assessed for difference in the diagnostic confidence in between Silent MRA from DSA and TOF MRA from DSA each of the CCF components. The mean diagnostic confidence score for the 37 cases was lower on TOF than Silent MRA as compared to DSA. But the Wilcoxon signed rank test revealed no significant difference between the diagnostic scoring for arterial detection for both Silent and TOF MRA. However, the difference between the scores for detecting fistulous point and venous drainage identification was statistically significant with reported difference in the mean score from DSA of only 0.36 on Silent as to 0.94 for TOF in fistulous point detection and 0.19 for Silent and 0.76 for TOF for venous visualization.

ILLUSTRATIVE CASES

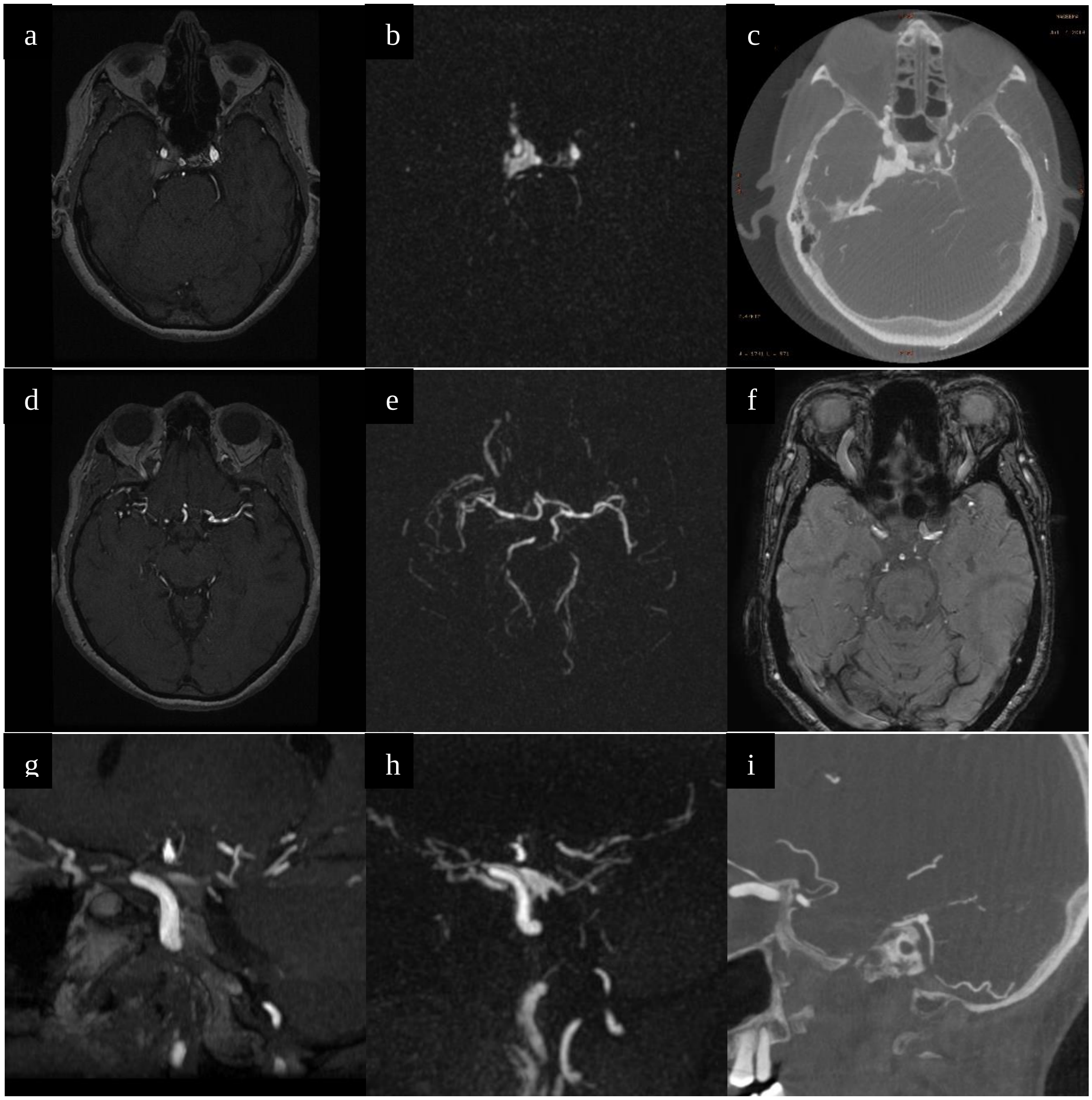

Case 1. Figure 1: 53-year-old female, case of right CSDAVF. (a,d,g- TOF MRA; b,e,h- Silent MRA; d- SWAN; c,i- DSA).1st row: Shunted pouch is located posteromedially to the cavernous sinus, in Silent MRA(b), TOF MRA(a) and 3D RA(c). 2nd row: On unenhanced 3T MRA images, visualization of vessel structures depends on their orientation relative to the scan plane. SOV venous drainage is better visualized in silent MRA(e) and SWAN (f), than TOF MRA (d). 3rd row: Superior petrosal sinus venous drainage (i- 3D RA) is also better visualized in Silent MRA(h), compared to TOF MRA(g).

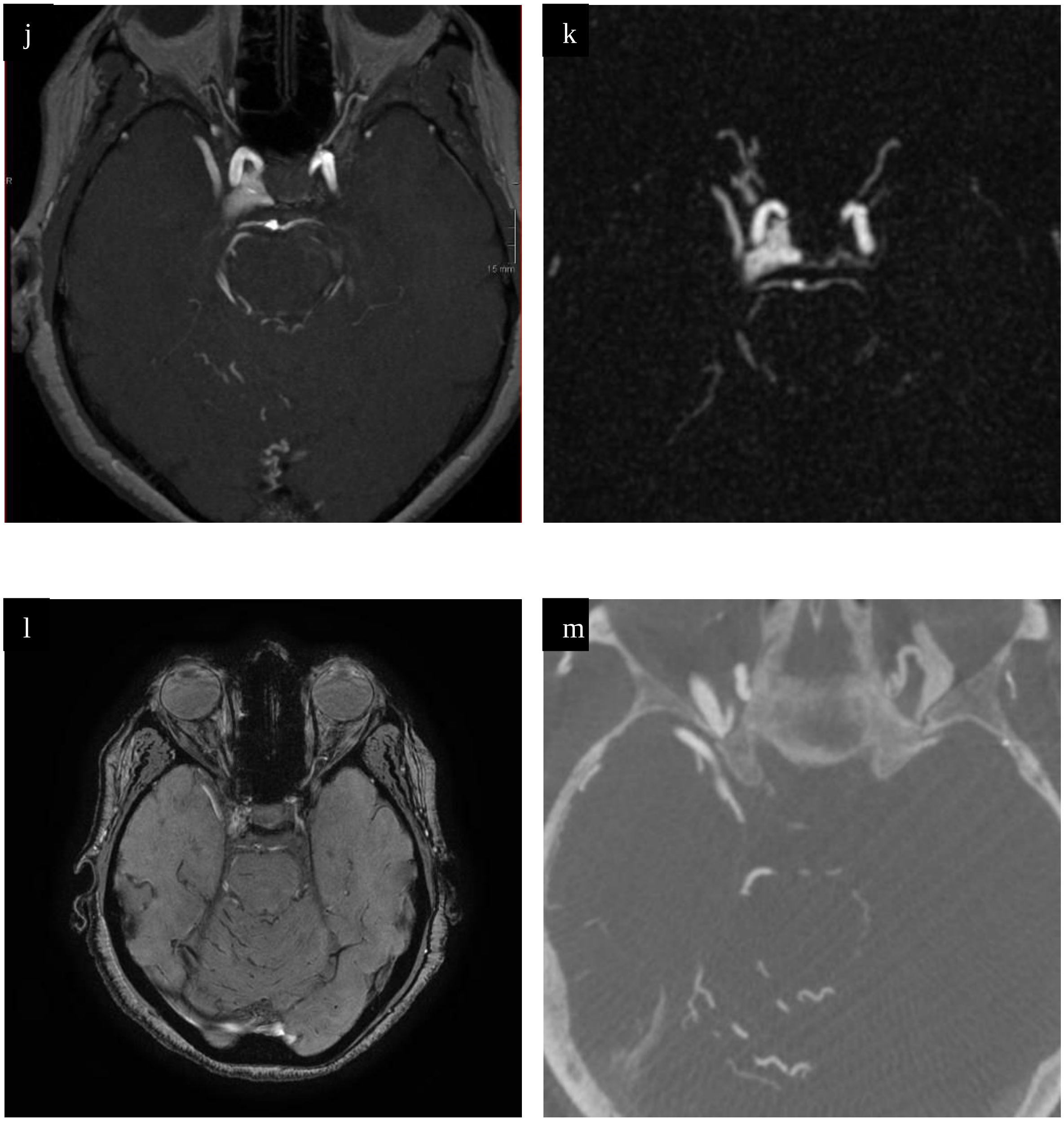

Case 1. Figure II: 53-year-old female, case of right CSDAVF. Superficial middle cerebral venous drainage (SMCV) on right side along with posterior fossa venous drainage in TOF MRA(j); Silent MRA(k); SWAN (l); and DSA (m).

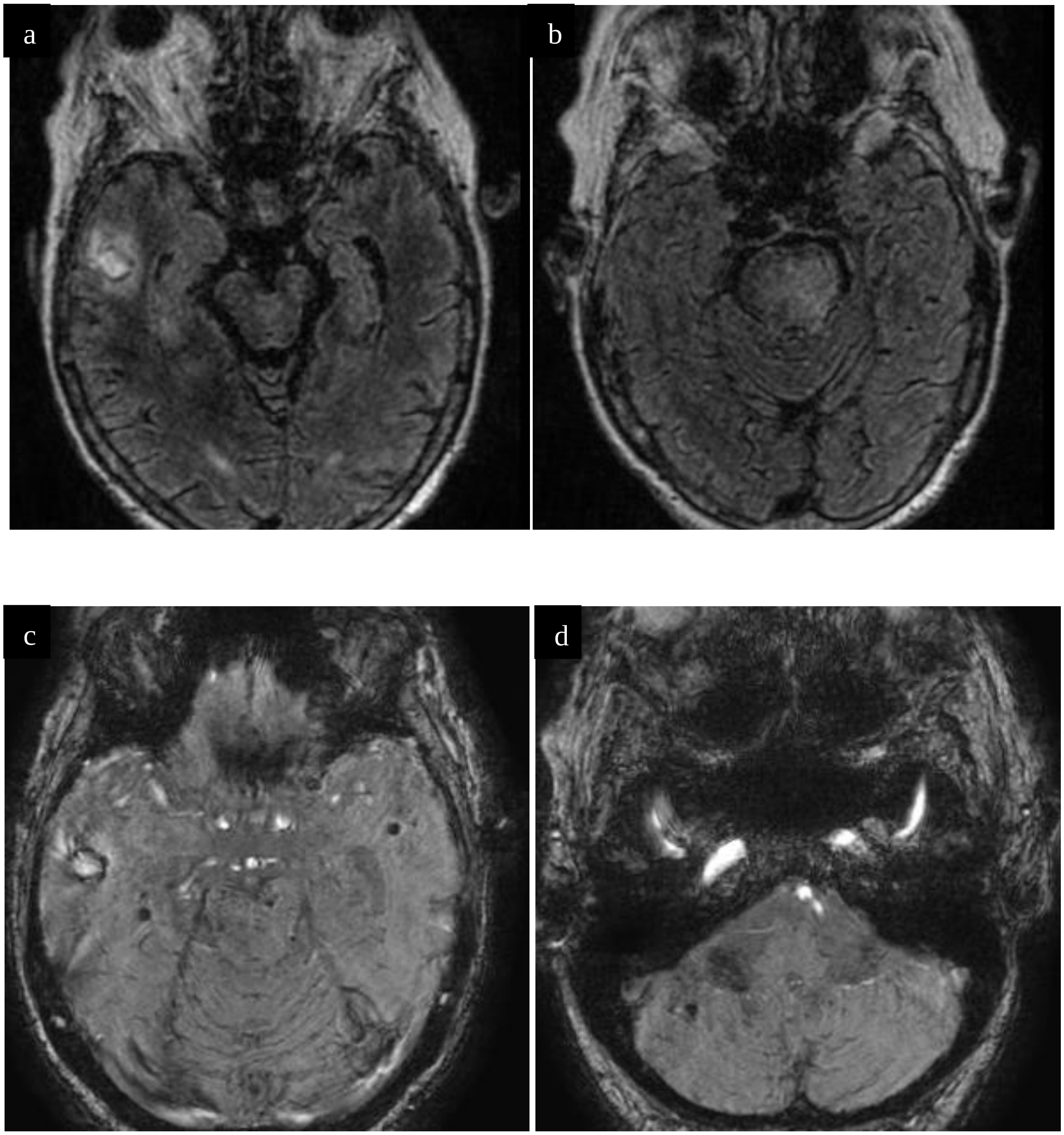

Case 2: 80-year-old female, case of right CS DAVF. Figure 1- FLAIR axial images (a,b) show right temporal bleed with pontine hyperintensity suggestive of ischemia/ edema. SWAN axial images show (c,d) multiple microbleeds in bilateral temporal lobes and cerebellum.

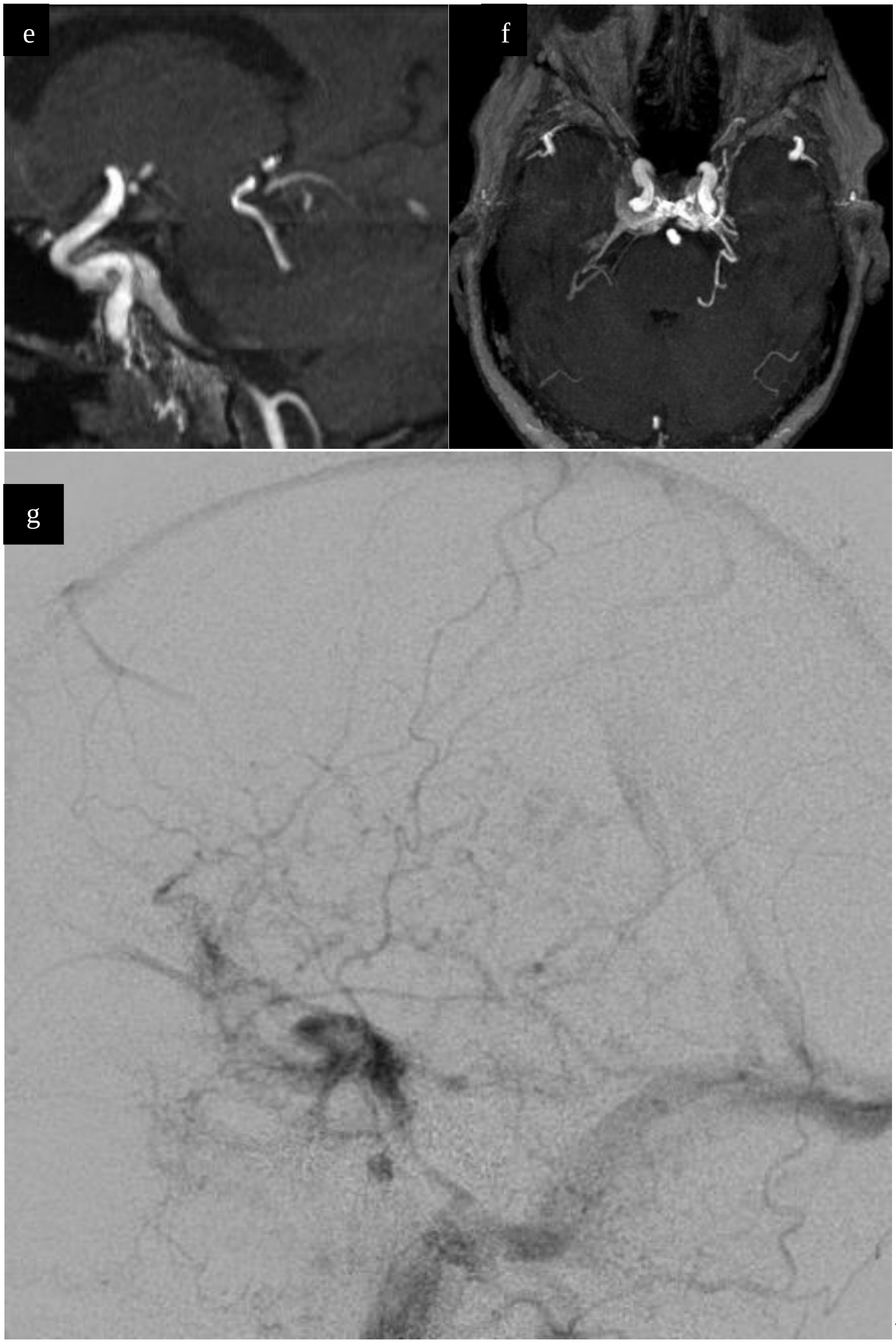

Case 2: Figure 2- 3D TOF MRA (e- sagittal) shows right inferior petrosal sinus (IPS) venous drainage; (f- axial)- right SPS venous drainage. g- DSA- lateral projection depicting deep venous drainage into brainstem veins through SPS and into basal vein of Rosenthal through SMCV.

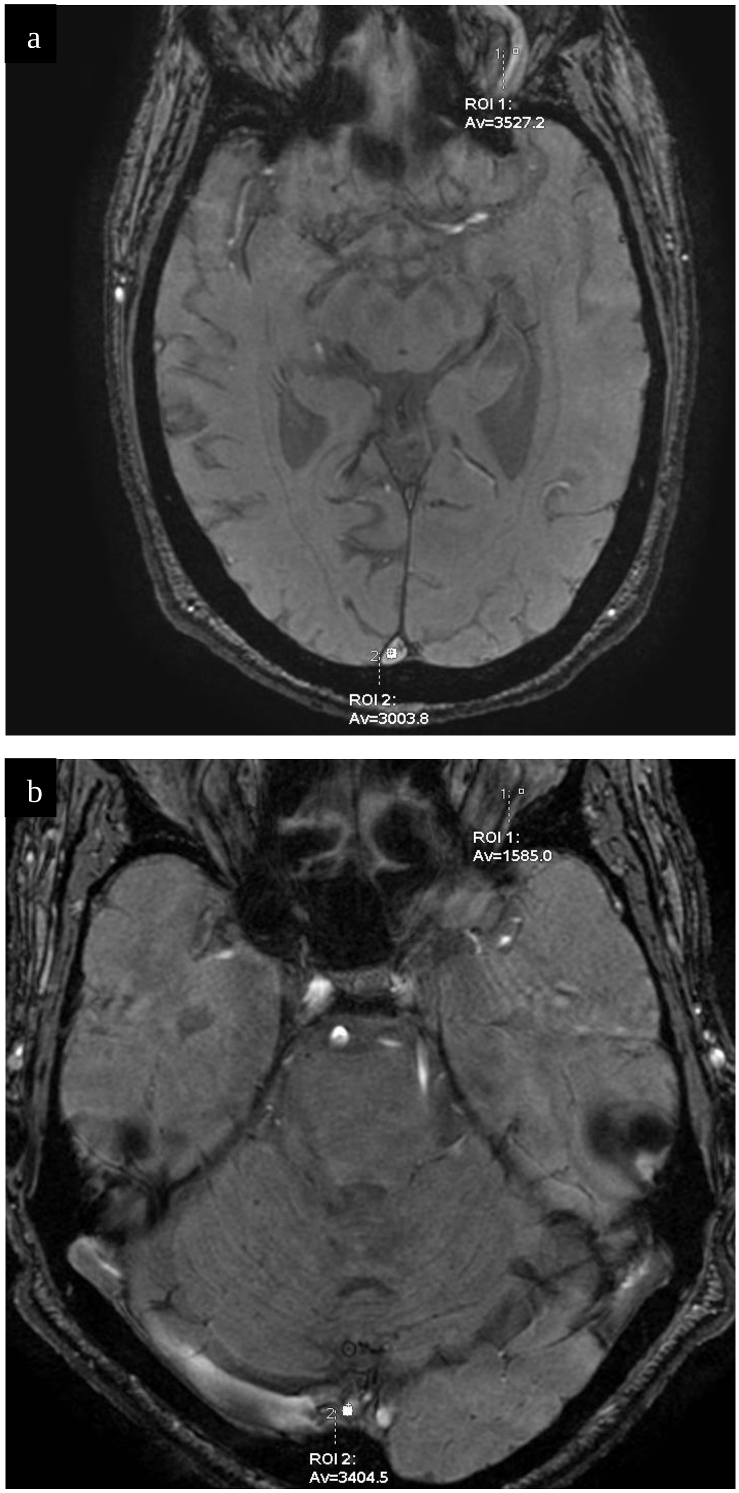

Case 3: Figure (a). Case of left CSDAVF. (b) Control. Shows the placement of region-of-interest (RoI) on the superior ophthalmic vein and in the superior sagittal sinus on magnitude images of SWAN sequence to measure the signal intensity ratio.

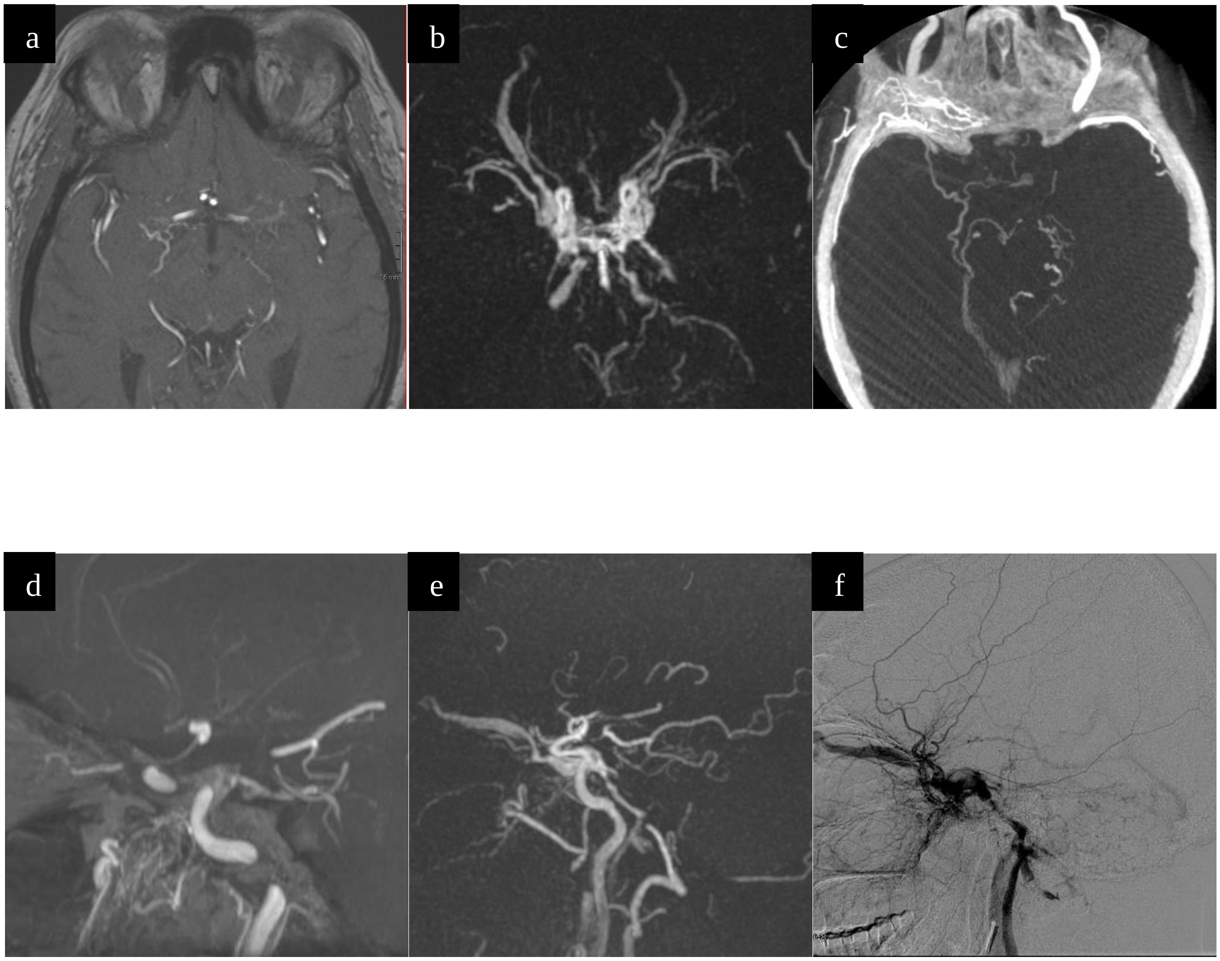

Case 4: Figure 1. Case of left CS DAVF. a,d- TOF MRA. b,e- Silent MRA. c,f- DSA. a,b,c -Shows bilateral SOV drainage with CVR into SMCV and Basal vein of Rosenthal. d,e,f- Inferior petrosal sinus drainage, better seen on Silent MRA than TOF MRA.

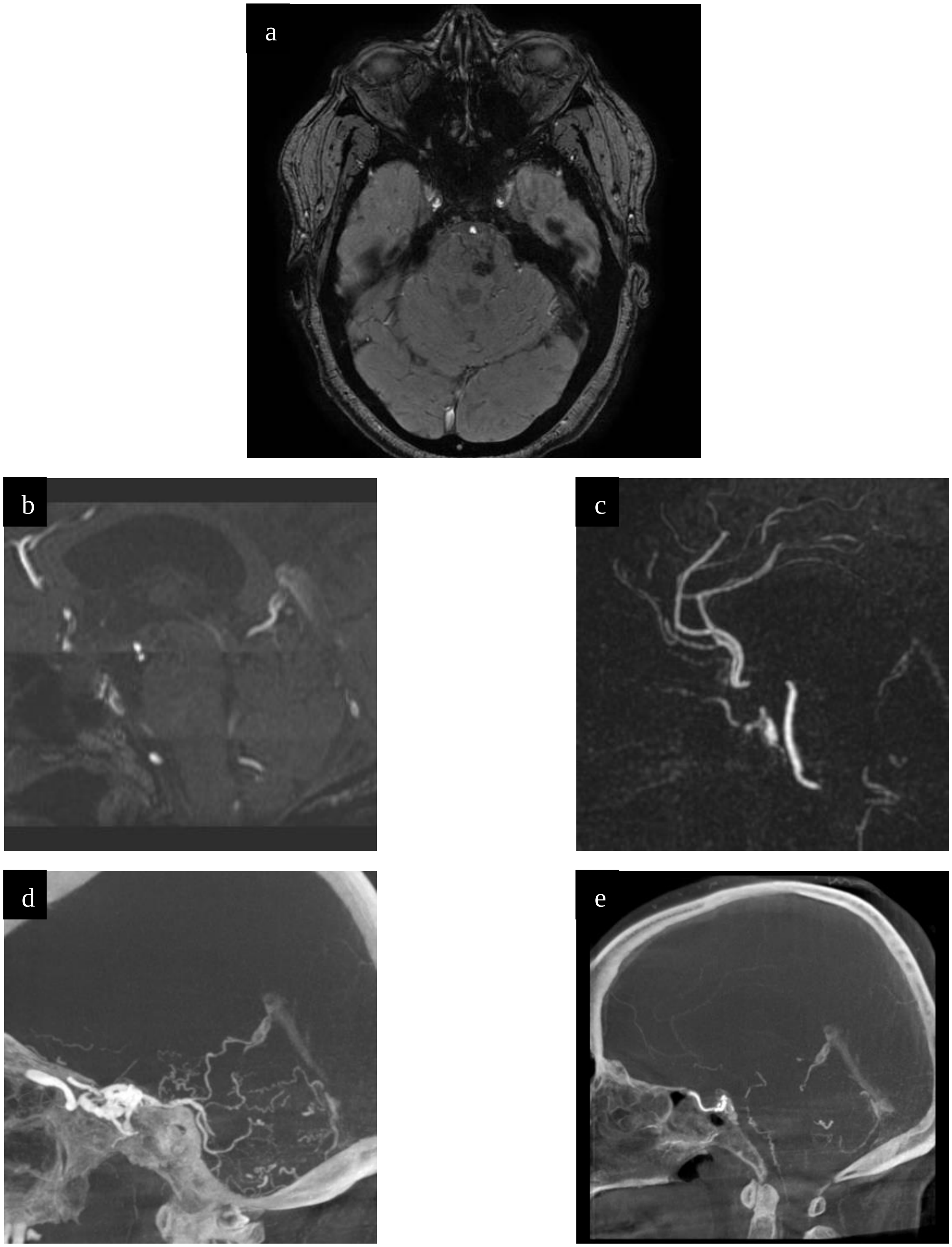

Case 4: Figure 2. Case of left CS DAVF. a- SWAN axial images show left hemipontine bleed; b (TOF MRA), c (Silent MRA), d,e (3D RA) shows posterior venous drainage into pontomesencephalic veins and into basal venous drainage.

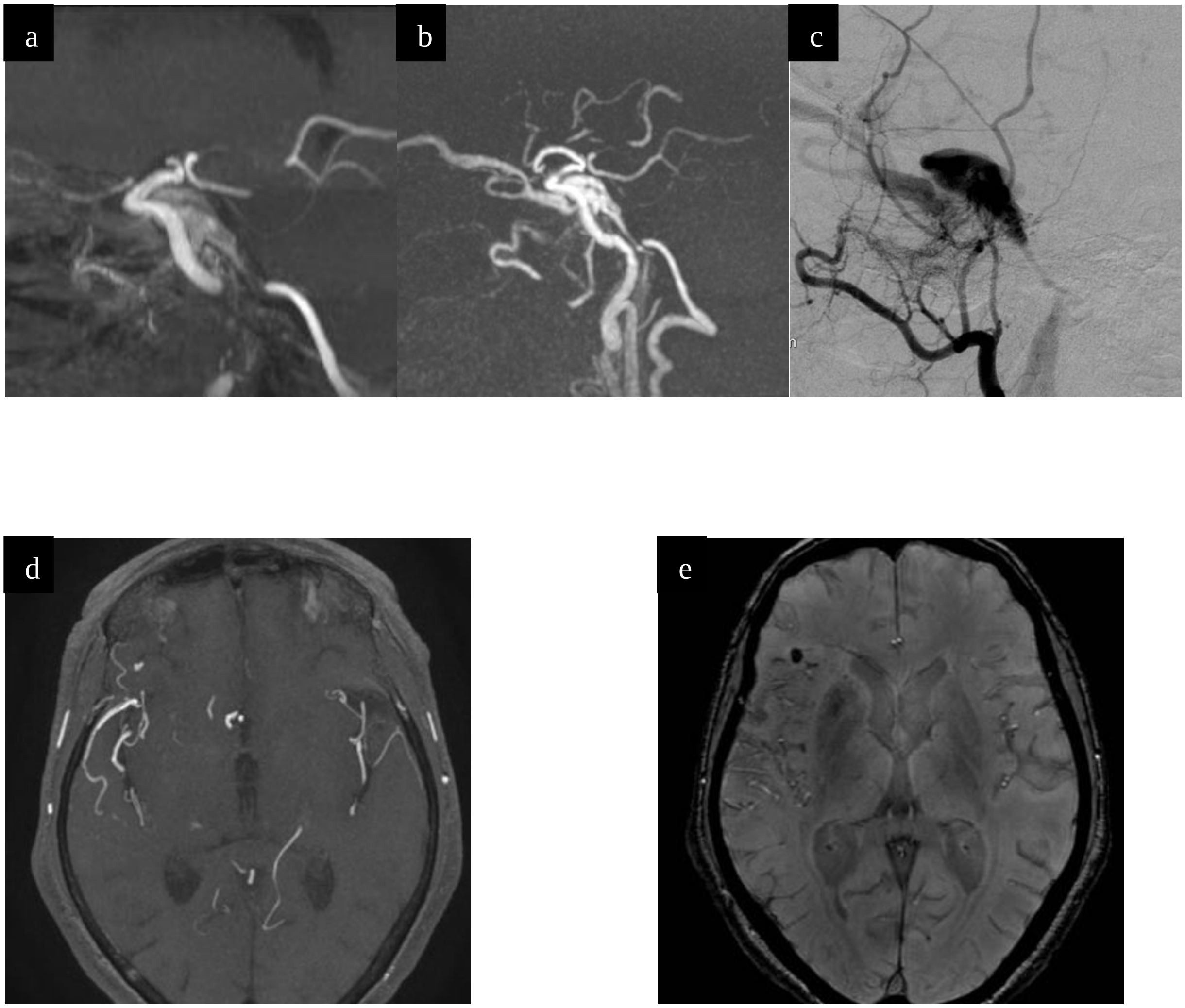

Case 5: Case of left CS DAVF. a, b c- TOF, Silent MRA and DSA images showing left dural CCF fed by branches of IMA and MMA, with SOV and IPS venous drainage. d (TOF MRA axial) shows right SMCV venous drainage with SWAN (e) showing microbleeds in the right frontal lobe.

DISCUSSION:

Our study evaluated whether advanced MRI sequences could be used as a reliable noninvasive diagnostic modality and in noninvasive follow up of patients with intracranial CSDAVF.

The study included a total of 37 patients (6 males and 31 females; age range 45 - 80 years; mean [SD] 59.5 ± 9.5 years). 67 % (25 patients) of the cases were in the age group of 50 to 70 years. This is similar to one of the largest published retrospective evaluation of 135 consecutive patients by Meyers et al where patient age ranged from 18 to 87 years, with a mean age of 60 ± 1.6 (mean± standard error) years. The male to female ratio (1:5) in our study showed a female preponderance. This is in concordance with previously published literature which has shown female preponderance of dural CSDAVF. The most prevalent sign was conjunctival injection followed by proptosis and the least prevalent was seizures, which was seen in one patient. This is similar to two large series by Meyers(58) and Stiebel Kalish et al(59). The clinical presentation of dural CCF in various series is shown in Table below.

Clinical Features	Meyers et al. (2002) % of 135	Stiebel-Kalish et al. (2002) % of 85	Kim (2006)(60) % of 65	Theaudin et al. (2006)(61) % of 27
Conjunctival injection	93	76	-	41
Chemosis	87	21	32	37
Proptosis	82	76	21	37
Diplopia	68	-	34	45
Decreased visual acuity	31	-	13	-
Headache/retroorbital pain	34	-	34	-
Retinal hemorrhage	-	18	-	30
Raised IOP	34	72	21	-

Most patients presented with orbital symptom pattern (86.4 %). Cavernous symptoms were noted in 75% of patients. 59% of patients presented with ocular pattern and 24% with cerebral pattern. In the series by Suh et al of 58 patients 53% the patients had orbital pattern, 71% had cavernous pattern, 64% had Ocular pattern and 5% had cerebral pattern(28).

As far as angioarchitecture features are concerned, most of the CSDAVF in our series were of Barrows Type D (92%) followed by Type C (5%) and Type B (3%). In a study by Debrun et al out of 32 patients of dural CCF there were 28 patients (87%) with Type D and 4 patients (13%) with Type C while no patient had Type B fistula(15). In the series of Barrow et al there were six patients with Type D fistula, 5 had Type B and 2 Type C fistulas(1). Our series has shown that Type D fistula which has feeders from both dural branches of ICA and ECA are the most common type of dural CCF as shown in previous studies.

There were 16 (43%) cases with the right, 18 (49%) cases with left and three (8%) cases with bilateral CCF. On retrospective evaluation with 3D rotational angiography, bilateral CCF was seen in only one patient, the other two cases had fistulous point in the midline/ intercavernous sinus location, mimicking bilateral CCF. A recent article has found a total of 35 reported cases of spontaneous, nontraumatic bilateral CCFs since 1963. There have been only six reported cases of bilateral type D fistulas in the literature out of the 35 reported cases of bilateral CCFs(62).

15(40%) patients had proliferative pattern, 13(35%) had restrictive pattern and 9(25%) had late restrictive pattern. In the series by Suh et al 40%, 40% and 20% of patients were found to have proliferative, restrictive and late restrictive patterns respectively(28).

Our study showed that differences in the presenting symptom patterns were related to the venous drainage patterns. CavSxP was related to the presence of posterior venous drainage

(*P*=0.041) and CerSxP to the SMCV drainage (P=0.001) and cortical venous reflux (P= 0.004). Suh et al also reported a relationship between presenting symptom patterns and the venous drainage pattern, that OrbSxP was related to the superior ophthalmic venous drainage and CavSxP to the inferior petrosal sinus and posterior fossa venous drainages.

The difference in the venous drainage was related to the presenting type differences because venous drainage pattern was partly included in defining each type. Absence of IPS venous drainage and presence of deep venous drainage is significantly associated with late restrictive type.

The angiographic types were also correlated to the presenting Sx patterns by Suh et al. They reported that PT and RTs were related to OrbSxP and CavSxP in contrast to LRT to OcuSxP . PT was related to the absence of OrbSxP in contrast to RT, which was related to the presence of CavSxP. However, in our study no significant difference noted in the presenting symptoms according to the angiographic types.

In the identification of the Suh type, the TOF MRA was concordant with DSA in 75 % (28) of the cases (Kappa =0.66; $p<0.001$). The discordance was more with the restrictive and late restrictive pattern. Silent MRA was concordant with DSA in 31 cases (83%), with a Kappa value of 0.75; $p<0.01$.

Location of fistula:

In 1970, Newton and Hoyt reviewed the angioarchitecture of 11 cases of CSDAVFs circumstantially by conventional angiography and demonstrated arteriovenous shunts adjacent to or within the wall of the cavernous sinus and located in the posterior compartment of the cavernous sinus in most cases(18). Takahashi et al. reported that most fistulous points of CSDAVFs were detected in the posterior portion of the cavernous sinus or in the posterior portion of the intercavernous sinus by contrast-enhanced MR imaging(63). The utility of CT like reconstructions of 3D rotational angiography in evaluating angioarchitecture of DAVFs has also been reported(64).

Kiyouse et el. evaluated shunted pouches and feeding arteries by high-resolution cross-sectional images and 3D images reconstructed from a rotational angiography dataset which are superior to 2D DSA in assessing small vascular structures such as perforating arteries. They could clearly demonstrate the shunted pouches to which multiple feeding arteries converge without overlapping of vessels and reported that the shunted pouches were most frequently located posteromedially to the cavernous sinus. The frequent location of "posteromedial" shunted pouches and their main feeding arteries of CSdAVFs may be due to the ventral epidural nature of the cavernous sinus as described by Geibprasert et al(65). Selective embolization of the shunted pouch or a compartment of the cavernous sinus is advantageous in that it allows the reduction of shunt flow using a small number of coils without increasing the pressure in venous outflow(17).

Our study revealed that most common site of fistula being posteromedial location (45%), followed by postero lateral location (26%), anterior (16%) and midline or intercavernous sinus location (13%). In four patients site of the fistula could not be made out clearly. Our findings are similar to the results published by Kiyouse et al and Kannath et al, with posteromedial being the commonest location followed by posterolateral location(17,50).

In the detection of the site of fistula, the TOF MRA was concordant with DSA in 75 % (28) of the cases (Kappa =0.66; $p<0.001$). The discordance was more with the detection of the location in the midline or intercavenrous sinus, which was mistaken for posteromedial CS in 3 cases. Silent MRA was concordant with DSA in 32 cases (86%), with a Kappa value of 0.82; $p<0.01$.

Venous drainage and CVR:

Cortical venous reflux into cortical veins through SMCV, Basal vein of Rosenthal and perimesencephalic veins were seen in 22 patients (59%). Deep venous and pontomedullary venous reflux were seen in 17 patients, with primary venous connection through superior petrosal sinus in 8 patients, and through uncal and bridging veins in rest of the patients.

CS DAVFs rarely cause venous ischemia (VI) and/or ICH despite the presence of CVD. Incidence of VI/ICH is reported 0% to 10(74) %. In series of Suh et al., 24 of 58 patients had CVDs, and three presented with VI/ICH(28). In a study by Miyamoto et al, 27 of 54 patients had CVDs, and six presented with VI/ICH(66). As per the literature associated risk of intracranial hemorrhage is relatively low compared to patients with DAVFs in other locations, especially at the tentorial sinus or in the anterior cranial fossa. The following table shows the frequency of cortical/leptomeningeal venous drainage(C/LVD) and associated hemorrhage in the literature.

STUDIES	Dural CCF	C/LVD	Hemorrhage
Halbach et al 1987	30	3(10%)	-
Awad et al 1990	45	NA	NA
Cognard et al 1995	33	4(12%)	0
Tomsick 1997	50	8(16%)	0
Satomi et al 2005	65	17(26.1%)	1(1.5%)
Theaudin et al 2006	27	5(18.5%)	0
Stiebel Kalish et al 2002	88	22(26%)	2(2.2%)
Meyers et al 2002	135	41(31%)	2(1.5%)

Microbleeds were noted in 9 cases (24%) out of 37 patients in this study. Microbleeds were commonly seen in the temporal lobes, followed by fronto-parietal lobes and cerebellum. Two patients had pontine hyperintensities in FLAIR MRI suggesting ischemia/ venous congestion. Microbleeds and venous congestion were significantly related to presence of SMCV venous drainage ($P<0.01$) and Cortical venous reflux ($P=0.002$). Though the presence of venous ischemia or edema has been reported in previous studies (pontine congestion), our study showed presence of microbleeds in SWAN sequence in the fronto-parietal lobes and cerebellum especially in patients with CVR, which was not reported earlier. Postulated reason for the occurrence of microbleeds in patients with CVR is the presence venous congestion and associated venous hypertension.

ADVANCED MRI SEQUENCES:

Arterial feeder characterization and detection:

In a study by Hirai et al, the sensitivity, specificity, and positive predictive value of source images from TOF MRA in revealing residual or recurrent CSDAVF were 100%, 80%, and 90%, respectively(41)**.** In our study the TOF MRA correctly identified 188 (89.5%) of the 210 arteries which were feeding the fistula and confirmed on DSA. Silent MRA correctly identified 195 (92.8%) of the 210 arterial feeders. The percentage of feeding arteries which were missed on Silent MRA and TOF were 7.2% for Silent MRA (15 feeders) and 10.5 % (22 feeders) for TOF MRA. Intermodality agreement for TOF MRA is kappa= 0.59 with DSA and for Silent MRA with DSA is k= 0.71. In a study by Azuma et al, very good to excellent agreement between 3T TOF MRA and DSA for the diagnosis of DAVF (fistula sites 0.968, 95% CI, 0.906 to 1.000; main feeders

0.809, 95% CI, 0.598 to 1.000; venous drainage 0.837, 95% CI, 0.660 to 1.000) indicated the reliability of unenhanced 3T MRA for gross characterization of DAVFs.(4)

Due to magnetic field inhomogeneity of the skull base, SWAN images were not evaluated for detecting arterial feeders and fistulous point.

VENOUS DRAINAGE IDENTIFICATION:

Totally 74 draining venous channels were identified on DSA in the 37 cases of CSDAVF assessed in this study. Of these 90 % were correctly identified on Silent MRA as to 85% identified on TOF and 71% in SWAN. Silent MRA was better in identification of both CVR and deep venous drainage with sensitivity of 90% and 81 % for Silent and TOF for detecting CVR and 82% vs 64.7% for deep venous visualization. The higher sensitivity of Silent MRA could be attributable to the high venous signal intensity and greater venous visualization. The lower venous detection on TOF especially for deep venous visualization was probably related to multi slab acquisition of TOF. This would result in some degree of signal loss in intervening regions between the acquisition slabs corresponding to level of the deep venous system in most of our cases. TOF MRA may also show low signal intensity due to the saturation effect of slow flow and inclination of SOV parallel to TOF saturation band while SWAN shows high signal intensity indicating the superiority of SWI over TOF MRA in detecting anterior SOV drainage(43).

In our study, 86% of cases with CVR could be identified and there was good intramodality agreement with kappa value of 0.78. This suggests that SWAN could be a reliable tool in identifying CVR. Jain et al demonstrated that SWI could correctly identify 75% of fistulous points and 90% cases with CVR with sensitivity of 85%. They also acknowledged the limitation of fistula site and CVR identification in vicinity of susceptibility artifacts (5). Similarly, in our study due to magnetic field inhomogeneity of the skull base, SWAN has low sensitivity in detecting posterior venous through SPS and IPS.

Diagnostic confidence scores for CSDAVF components:

The mean diagnostic confidence score for the 37 cases was lower on TOF than Silent MRA as compared to DSA. But the Wilcoxon signed rank test revealed no significant difference between the diagnostic scoring for arterial detection for both Silent and TOF MRA indicating both to have a similar efficacy in arterial feeder identification in AVM. However, the difference between the scores for detecting fistulous point and venous drainage identification was statistically significant with reported difference in the mean score from DSA of only 0.36 on Silent as to 0.94 for TOF in fistulous point detection and 0.19 for Silent and 0.76 for TOF for venous visualization.

3T MRA protocol offers some benefits over that with 1.5T. The SNR of 3T scanners is approximately twice that of 1.5T instruments, and the spatial resolution is higher. These techniques yielded high spatial resolution, which allowed the depiction of small feeders and venous drainages. Axial source, MIP, and partial MIP MRA images were used to evaluate vessel structures. Although DSA like images are derived from the MIP algorithm, vessels exhibiting lower signal intensity may be lost and small or slow-flowing vessels may not be visualized. Not all arteries usually visible on DSA were visualized on 3T MRA images. Vessel diameter can be small compared with the voxel size of MRA images, and their spatial resolution is insufficient for their depiction. Also, visualization of vessel structures depends on their orientation relative to the scan plane. If it is parallel to flowing blood, enhancement may be lost as spins are exposed to saturating radiofrequency pulses. However, our current study demonstrated very good agreement between 3D TOF MRA and DSA findings for the main arterial feeders(4).

Silent-MRA may better visualize fine and slow-flow vessels, because it is insensitive to saturation effects and is not influenced by vessel direction, with improved venous signal. Inferiority of both SNR and CNR is a major disadvantage of silent-MRA. Increased acquisition time is also another disadvantage of silent-MRA but does not seem clinically problematic. As a disadvantage in silent-MRA, the source images provide poor anatomical information due to low signal intensity in the background(67). TOF-MRA can depict much more anatomical information in comparison of silent-MRA, which could be overcome by fusing volumetric images over the Silent MRA.

SWAN is reliable in detecting CVR with improved sensitivity, with additional finding of silent microbleeds in patients with cortical venous reflux. Inclusion of this sequence in the MR protocol provides unique information regarding the morphological and hemodynamic characteristics of the CSDAVF and thus improves the diagnostic accuracy of MRI

In assessing main arterial feeders, intermodality agreement is better for both 3D TOF MRA and Silent MRA. With regard to fistula and venous drainage, intermodality agreement is better for Silent MRA than 3D TOF MRA.

LIMITATIONS:

Our data were based on a single-center study, and the number of patients was relatively small.

Interrater variability was an entity not assessed in this study, which would have assessed the reliability in assessment of angiomorphology in each of these modalities.

Only patients with a proven diagnosis of CSDAVF were included in the study analysis and hence the investigators were aware of the presence of a fistula and may have been biased.

CONCLUSION:

In conclusion, dural CCFs most commonly affect elderly women, and ocular symptoms and signs are the most frequent clinical finding. The fistula is more commonly supplied by multiple arterial feeders from the ICA, ECA or both, and cortical venous reflux is not rare.

The arterial feeder identification was similar on both the TOF and Silent MRA, but with better diagnostic confidence for Silent MRA.

For both fistulous point and venous detection Silent MRA outperformed TOF MRA. This can be attributed to the better venous visualization on silent MRA.

SWAN is reliable in detecting CVR with improved sensitivity, with additional finding of silent microbleeds, especially in patients with cortical venous reflux.

This study also demonstrated a good intermodality agreement in identification of arterial feeders, fistula site, venous drainage and CVR for 3D TOF MRA, Silent MRA and SWAN with that of the gold standard DSA.

Even though the results of this study are encouraging, MRI cannot replace DSA while planning treatment. On the other hand, given these results the benefits of using this modality as the follow-up method where repeated angiograms may be needed, instead of DSA is a better alternative considering that dural CCF patients are typically older and some of them with significant vascular risk factors.

BIBLIOGRAPHY:

1. Barrow DL, Spector RH, Braun IF, Landman JA, Tindall SC, Tindall GT. Classification and treatment of spontaneous carotid-cavernous sinus fistulas. J Neurosurg. 1985 Feb;62(2):248–56.

2. Kaufmann TJ, Huston J, Mandrekar JN, Schleck CD, Thielen KR, Kallmes DF. Complications of diagnostic cerebral angiography: evaluation of 19,826 consecutive patients. Radiology. 2007 Jun;243(3):812–9.

3. Willinsky RA, Taylor SM, TerBrugge K, Farb RI, Tomlinson G, Montanera W. Neurologic complications of cerebral angiography: prospective analysis of 2,899 procedures and review of the literature. Radiology. 2003 May;227(2):522–8.

4. Azuma M, Hirai T, Shigematsu Y, Kitajima M, Kai Y, Yano S, et al. Evaluation of Intracranial Dural Arteriovenous Fistulas: Comparison of Unenhanced 3T 3D Time-of-flight MR Angiography with Digital Subtraction Angiography. MRMS. 2015;14(4):285–93.

5. Jain NK, Kannath SK, Kapilamoorthy TR, Thomas B. The application of susceptibility-weighted MRI in pre-interventional evaluation of intracranial dural arteriovenous fistulas. J NeuroIntervent Surg. 2017 May;9(5):502–7.

6. Kesavadas C, Gupta A, George U, Jolappara M. Susceptibility-weighted imaging in the evaluation of brain arteriovenous malformations. Neurol India. 2010;58(4):608.

7. Hodel J, Gerber S, Zins M, Rodallec M, Leclerc X, Blanc R, et al. MR Imaging Findings in Intracranial Dural Arteriovenous Fistula Shunt with Retrograde Cortical Venous Drainage Using Susceptibility-Weighted Angiography. AJNR Am J Neuroradiol. 2011 Nov;32(10):E196–7.

8. Moon JI, Baek HJ, Ryu KH, Park H. A novel non-contrast-enhanced MRA using silent scan for evaluation of brain arteriovenous malformation: A case report and review of literature. Medicine. 2017 Nov;96(45):e8616.

9. Yeung S, Suen SS, Yu SC, Lao TT, Leung T, Lau T. Spontaneous carotid cavernous fistula complicating pregnancy. Hong Kong Med J. 2013 Jun 4;19(3):258–61.

10. Miller NR. Dural Carotid-Cavernous Fistulas: Epidemiology, Clinical Presentation, and Management. Neurosurgery Clinics. 2012 Jan 1;23(1):179–92.

11. Harris FS, Rhoton AL. Anatomy of the cavernous sinus: A microsurgical study. Journal of Neurosurgery. 1976 Aug 1;45(2):169–80.

12. Thomas AJ, Chua M, Fusco M, Ogilvy CS, Tubbs RS, Harrigan MR, et al. Proposal of Venous Drainage–Based Classification System for Carotid Cavernous Fistulae With Validity Assessment in a Multicenter Cohort. Neurosurgery. 2015 Sep 1;77(3):380–5.

13. Martins C, Yasuda A, Campero A, Ulm AJ, Tanriover N, Rhoton A. Microsurgical Anatomy of the Dural Arteries. Oper Neurosurg (Hagerstown). 2005 Apr 1;56(suppl_4):ONS-211-ONS-251.

14. Henderson AD, Miller NR. Carotid-cavernous fistula: current concepts in aetiology, investigation, and management. Eye. 2018 Feb;32(2):164–72.

15. Debrun GM, Viñuela F, Fox AJ, Davis KR, Ahn HS. Indications for Treatment and Classification of 132 Carotid-Cavernous Fistulas. Neurosurgery. 1988 Feb 1;22(2):285–9.

16. Suh DC, Lee JH, Kim SJ, Chung SJ, Choi CG, Kim HJ, et al. New Concept in Cavernous Sinus Dural Arteriovenous Fistula: Correlation With Presenting Symptom and Venous Drainage Patterns. Stroke. 2005 Jun;36(6):1134–9.

17. Kiyosue H, Tanoue S, Hori Y, Hongo N, Mori H. Shunted pouches of cavernous sinus dural AVFs: evaluation by 3D rotational angiography. Neuroradiology. 2015 Mar;57(3):283–90.

18. Newton TH, Hoyt WF. Dural arteriovenous shunts in the region of the cavernous sinus. Neuroradiology. 1970 Aug 1;1(2):71–81.

19. Takahashi M, Nakano Y. Magnification angiography of dural carotid-cavernous sinus fistulae with emphasis on clinical and angiographic evolution. Neuroradiology. 1980;19(5):249–56.

20. Pang D, Kerber C, Biglan AW, Ahn HS. External Carotid-Cavernous Fistula in InfancyCase Report and Review of the Literature. Neurosurgery. 1981 Feb 1;8(2):212–8.

21. Luo C-B, Teng MM-H, Chang F-C, Chang C-Y. Traumatic indirect carotid cavernous fistulas: angioarchitectures and results of transarterial embolization by liquid adhesives in 11 patients. Surg Neurol. 2009 Feb;71(2):216–22.

22. Gao B-L, Zhao W, Xu G-P. The Development of a De Novo Indirect Carotid-Cavernous Fistula After Successful Occlusion of Bilateral Direct Carotid-Cavernous Fistulas. The Journal of Trauma: Injury, Infection, and Critical Care [Internet]. 2009 Feb 1 [cited 2019 Jul 20];66(2). Available from: insights.ovid.com

23. Grove AS. The Dural Shunt Syndrome: Pathophysiology and Clinical Course. Ophthalmology. 1984 Jan 1;91(1):31–44.

24. Ringer AJ, Salud L, Tomsick TA. Carotid cavernous fistulas: anatomy, classification, and treatment. Neurosurgery Clinics of North America. 2005 Apr 1;16(2):279–95.

25. Nomura M, Mori K, Tamase A, Kamide T, Seki S, Iida Y, et al. Cavernous Sinus Dural Arteriovenous Fistula Patients Presenting With Headache as an Initial Symptom. J Clin Med Res. 2016 Apr;8(4):342–5.

26. Miller NR. Article--Diagnosis and management of dural carotid–cavernous sinus fistulas. Neurosurgical Focus. 2007 Nov 1;23(5):E13.

27. Woolen S, Gemmete JJ, Pandey AS, Chaudhary N. Dural carotid-cavernous fistula presenting with confusion and expressive aphasia. J Clin Neurosci. 2015 Nov;22(11):1844–6.

28. Suh DC, Lee JH, Kim SJ, Chung SJ, Choi CG, Kim HJ, et al. New Concept in Cavernous Sinus Dural Arteriovenous Fistula: Correlation With Presenting Symptom and Venous Drainage Patterns. Stroke. 2005 Jun;36(6):1134–9.

29. Benndorf G. Classification of Cavernous Sinus Fistulas (CSFs) and Dural Arteriovenous Fistulas (DAVFs). In: Benndorf G, editor. Dural Cavernous Sinus Fistulas: Diagnostic and Endovascular Therapy [Internet]. Berlin, Heidelberg: Springer Berlin Heidelberg; 2010 [cited 2019 Jul 23]. p. 51–63. (Medical Radiology). Available from: https://doi.org/10.1007/978-3-540-68889-1_4

30. Awad IA, Little JR, Akarawi WP, Ahl J. Intracranial dural arteriovenous malformations: factors predisposing to an aggressive neurological course. J Neurosurg. 1990 Jun;72(6):839–50.

31. Cognard C, Gobin YP, Pierot L, Bailly AL, Houdart E, Casasco A, et al. Cerebral dural arteriovenous fistulas: clinical and angiographic correlation with a revised classification of venous drainage. Radiology. 1995 Mar;194(3):671–80.

32. Klisch J, Huppertz HJ, Spetzger U, Hetzel A, Seeger W, Schumacher M. Transvenous treatment of carotid cavernous and dural arteriovenous fistulae: results for 31 patients and review of the literature. Neurosurgery. 2003 Oct;53(4):836–56; discussion 856-857.

33. Satomi J, Satoh K. [Epidemiology and etiology of dural arteriovenous fistula]. Brain Nerve. 2008 Aug;60(8):883–6.

34. Tsai LK, Jeng JS, Liu HM, Wang HJ, Yip PK. Intracranial dural arteriovenous fistulas with or without cerebral sinus thrombosis: analysis of 69 patients. J Neurol Neurosurg Psychiatry. 2004 Nov;75(11):1639–41.

35. Chung SJ, Kim JS, Kim JC, Lee SK, Kwon SU, Lee MC, et al. Intracranial dural arteriovenous fistulas: analysis of 60 patients. Cerebrovasc Dis. 2002;13(2):79–88.

36. Uchino A, Hasuo K, Matsumoto S, Masuda K. MRI of dural carotid-cavernous fistulas. Comparisons with postcontrast CT. Clin Imaging. 1992 Dec;16(4):263–8.

37. Hirabuki N, Fujita N, Hashimoto T, Fujii K, Miura T, Mitomo M, et al. Follow-up MRI in dural arteriovenous malformations involving the cavernous sinus: emphasis on detection of venous thrombosis. Neuroradiology. 1992 Sep 1;34(5):423–7.

38. Miyagishima T, Inoue M, Ohno H, Hasuo K, Hara T, Terano N, et al. Pontine venous congestion due to dural arteriovenous fistula of the cavernous sinus: Case report and review of the literature. Surg Neurol Int. 2012;3(1):53.

39. Uchino A, Kato A, Kuroda Y, Shimokawa S, Kudo S. Pontine venous congestion caused by dural carotid-cavernous fistula: report of two cases. Eur Radiol. 1997 Apr;7(3):405–8.

40. Chen CC-C, Chang PC-T, Shy C-G, Chen W-S, Hung H-C. CT angiography and MR angiography in the evaluation of carotid cavernous sinus fistula prior to embolization: a comparison of techniques. AJNR Am J Neuroradiol. 2005 Oct;26(9):2349–56.

41. Hirai T, Korogi Y, Hamatake S, Ikushima I, Sugahara T, Sigematsu Y, et al. Three-dimensional FISP imaging in the evaluation of carotid cavernous fistula: comparison with contrast-enhanced CT and spin-echo MR. AJNR Am J Neuroradiol. 1998 Feb;19(2):253–9.

42. Tsai Y-F, Chen L-K, Su C-T, Lu T-N, Wu C-C, Kuo C-J. Utility of Source Images of Three-Dimensional Time-of-Flight Magnetic Resonance Angiography in the Diagnosis of Indirect Carotid-Cavernous Sinus Fistulas. Journal of Neuro-ophthalmology. 2004 Dec 1;24(4):285–9.

43. Harsha KJ, Basti RS, Kesavadas C, Thomas B. Susceptibility-weighted imaging in carotido-cavernous fistulas. A case control study. Interv Neuroradiol. 2013 Dec;19(4):438–44.

44. Nakagawa I, Taoka T, Wada T, Nakagawa H, Sakamoto M, Kichikawa K, et al. The use of susceptibility-weighted imaging as an indicator of retrograde leptomeningeal venous drainage and venous congestion with dural arteriovenous fistula: diagnosis and follow-up after treatment. Neurosurgery. 2013 Jan;72(1):47–54; discussion 55.

45. Koktzoglou I, Meyer JR, Ankenbrandt WJ, Giri S, Piccini D, Zenge MO, et al. Nonenhanced arterial spin labeled carotid MR angiography using three-dimensional radial balanced steady-state free precession imaging. J Magn Reson Imaging. 2015 Apr;41(4):1150–6.

46. Irie R, Suzuki M, Yamamoto M, Takano N, Suga Y, Hori M, et al. Assessing Blood Flow in an Intracranial Stent: A Feasibility Study of MR Angiography Using a Silent Scan after Stent-Assisted Coil Embolization for Anterior Circulation Aneurysms. AJNR Am J Neuroradiol. 2015 May;36(5):967–70.

47. Takano N, Suzuki M, Irie R, Yamamoto M, Hamasaki N, Kamagata K, et al. Usefulness of Non–Contrast-Enhanced MR Angiography Using a Silent Scan for Follow-Up after Y-Configuration Stent-Assisted Coil Embolization for Basilar Tip Aneurysms. AJNR Am J Neuroradiol. 2017 Mar;38(3):577–81.

48. Oishi H, Fujii T, Suzuki M, Takano N, Teranishi K, Yatomi K, et al. Usefulness of Silent MR Angiography for Intracranial Aneurysms Treated with a Flow-Diverter Device. AJNR Am J Neuroradiol. 2019 May;40(5):808–14.

49. Lasjaunias PL. Anatomy of the tentorial arteries. J Neurosurg. 1984 Dec;61(6):1159–60.

50. Kannath SK, Rajan JE, Sarma SP. Anatomical localization of the cavernous sinus dural fistula by 3D rotational angiography with emphasis on clinical and therapeutic implications. J Neuroradiol. 2017 Sep;44(5):326–32.

51. Liu H, Wang Y, Chen Y, Cheng J, Yip P, Tu Y. Long-term clinical outcome of spontaneous carotid cavernous sinus fistulae supplied by dural branches of the internal carotid artery. Neuroradiology. 2001 Nov 1;43(11):1007–14.

52. Kai Y, Hamada J, Morioka M, Yano S, Kuratsu J. Treatment of cavernous sinus dural arteriovenous fistulae by external manual carotid compression. Neurosurgery. 2007 Feb;60(2):253–7; discussion 257-258.

53. Arat A, Saatci I, Ozgen B, Cekirge S. Transvenous injection of onyx for casting of the cavernous sinus for the treatment of a carotid-cavernous fistula. Neuroradiology. 2004;46(12):1012–5.

54. Gemmete J, Ansari S, Gandhi D. Endovascular Techniques for Treatment of Carotid-Cavernous Fistula. Journal of Neuro-ophthalmology. 2009 Mar 1;29(1):62–71.

55. Chen C-J, Mastorakos P, Caruso JP, Ding D, Schmitt PJ, Buell TJ, et al. Transorbital Approach for Endovascular Occlusion of Carotid-Cavernous Fistulas: Technical Note and Review of the Literature. Cureus. 2017 Jan 12;9(1):e976.

56. Henderson AD, Miller NR. Carotid-cavernous fistula: current concepts in aetiology, investigation, and management. Eye. 2018 Feb;32(2):164–72.

57. Chong GT, Mukundan S, Kirkpatrick JP, Zomorodi A, Sampson JH, Tariq Bhatti M. Stereotactic Radiosurgery in the Treatment of a Dural Carotid-Cavernous Fistula: Journal of Neuro-Ophthalmology. 2010 Jun;30(2):138–44.

58. Meyers PM, Halbach VV, Dowd CF, Lempert TE, Malek AM, Phatouros CC, et al. Dural carotid cavernous fistula: definitive endovascular management and long-term follow-up. American Journal of Ophthalmology. 2002 Jul 1;134(1):85–92.

59. Stiebel-Kalish H, Setton A, Nimii Y, Kalish Y, Hartman J, Huna Bar-On R, et al. Cavernous sinus dural arteriovenous malformations: Patterns of venous drainage are related to clinical signs and symptoms. Ophthalmology. 2002 Sep 1;109(9):1685–91.

60. Kim DJ, Kim DI, Suh SH, Kim J, Lee SK, Kim EY, et al. Results of Transvenous Embolization of Cavernous Dural Arteriovenous Fistula: A Single-Center Experience with Emphasis on Complications and Management. American Journal of Neuroradiology. 2006 Nov 1;27(10):2078–82.

61. Théaudin M, Saint-Maurice J, Chapot R, Vahedi K, Mazighi M, Vignal C, et al. Diagnosis and treatment of dural carotid–cavernous fistulas: a consecutive series of 27 patients. J Neurol Neurosurg Psychiatry. 2007 Feb;78(2):174–9.

62. Khan S, Gibbon C, Johns S. A rare case of bilateral spontaneous indirect caroticocavernous fistula treated previously as a case of conjunctivitis. Ther Adv Ophthalmol [Internet]. 2018 Jul 17 [cited 2019 Jul 23];10. Available from: https://www.ncbi.nlm.nih.gov/pmc/articles/PMC6050812/

63. Takahashi S, Sakuma I, Tomura N, Watarai J, Mizoi K. Transvenous Embolization of Dural Arteriovenous Fistula of the Cavernous Sinus: Fistulous Points and Route of Catheterization. Interv Neuroradiol. 2004 Mar;10(1_suppl):85–92.

64. Hiu T, Kitagawa N, Morikawa M, Hayashi K, Horie N, Morofuji Y, et al. Efficacy of DynaCT Digital Angiography in the Detection of the Fistulous Point of Dural Arteriovenous Fistulas. American Journal of Neuroradiology. 2009 Mar 1;30(3):487–91.

65. Geibprasert S, Pereira V, Krings T, Jiarakongmun P, Toulgoat F, Pongpech S, et al. Dural arteriovenous shunts: a new classification of craniospinal epidural venous anatomical bases and clinical correlations. Stroke. 2008 Oct;39(10):2783–94.

66. Miyamoto N, Naito I, Takatama S, Shimizu T, Iwai T, Shimaguchi H. Clinical and angiographic characteristics of cavernous sinus dural arteriovenous fistulas manifesting as venous infarction and/or intracranial hemorrhage. Neuroradiology. 2009 Jan;51(1):53–60.

67. Tomura N, Kokubun M, Horiuchi K, Watanabe Z. Comparison of TOF-MRA and silent scan-MRA in depicting cerebral arteries in patients with Moyamoya disease. Acta Radiol. 2019 Jan 25;028418511882478.

INFORMATION SHEET

<u>TITLE OF THE STUDY:</u> Imaging of Carotid-Cavernous Fistula – comparing advanced MRI sequences with Digital subtraction angiography.

<u>Study number:</u>

Participant's name: ____

Date of Birth / Age (in years): ________________________________

Son/daughter of ____

You ……………………………………………………………. have been informed that you have abnormal connections between blood vessels (arteries and veins) in the coverings of brain in the region of cavernous sinus (blood containing sac in the middle of skull base). If the condition is left untreated it may cause permanent loss of vision and sometimes haemorrhage in brain. For this you will have undergone or will be undergoing a digital subtraction angiography (DSA) test and Magnetic Resonance Imaging (MRI) as a part of clinical evaluation of your disease. This is to plan the treatment or for follow up your disease.

You are requested to participate in a study to evaluate the role of a new Magnetic Resonance Imaging sequences in Carotid-Cavernous Fistula. While participating in this study, only the imaging data from the MRI and DSA investigations you have undergone for your treatment purpose will be used. Participating in this study will in no way influence your treatment decisions. The benefit that you may incur from this study is, if this new MRI technique is found useful, during subsequent reviews/ follow up your further imaging follow up can be limited to just an MRI rather than performing an invasive evaluation like DSA.

What are DSA and MRI and do they have any harmful effects?

DSA (Digital subtraction angiography) test is an advanced imaging technique where the blood flow to your brain will be evaluated by injecting a dye into the arteries to the brain through a small tube which will be inserted through the artery in your thigh. X-Rays will be obtained during the procedure which will clearly show the abnormal connections between arteries and veins if they exist. You will not experience much pain as an injection will be given on your thigh prior to the procedure to make it numb. You will not feel any pain during the rest of the procedure. In rare cases some people may have allergic reaction to the dye. There is also a very small risk of injury to the blood vessel and slight chance of bleeding at site of puncture. This test is vital in diagnosis of your condition and is also the means of treatment if planned subsequently.

MRI is an advanced imaging technique which uses certain waves and magnetic fields to image body part. It does not involve any ionizing radiation. There will be no administration of any type of drug or medicine during the study. Some patients may develop claustrophobia (Fear of closed spaces etc.) due to closed space and noise. This investigation is not to be done for patient with metallic implants, pacemakers. This MRI is being done as a part of clinical evaluation of your disease; however certain data from this study will be used for research purpose to compare with the DSA study which you have already undergone/ will undergo shortly.

If you take part what will you have to do?

This study will only analyse the results of the routinely ordered imaging investigations you will undergo during treatment and follow up of your illness. You will not be required to do anything apart from the regular follow up that will be advised to you.

Can you withdraw from this study after it starts?

Your participation in this study is entirely voluntary and you are also free to decide to withdraw permission to participate in this study. If you do so, this will not affect your usual treatment at this hospital in any way.

What will happen if you develop any study related injury?

This study only analyses the results of your investigation and treatment details and thus we do not expect any injury to happen to you but if you do develop any side effects or problems due to the study, these will be treated at this institute by the experienced team of medical professionals. We are unable to provide any monetary compensation, however.

Will you have to pay for the study?

The study will only analyse the results of the investigations and treatment which you will undergo in natural process of your treatment for Carotid-Cavernous Fistula at this institute and no extra cost will be borne by you for this study.

What happens after the study is over?

You may or may not benefit from this study. If the study is found useful then during subsequent reviews you can be evaluated just by non-invasive MRI rather than undergo a more invasive DSA.

Will your personal details be kept confidential?

The results of this study may be published in a medical journal, but you will not be identified by name in any publication or presentation of results. However, your medical notes may be reviewed by people associated with the study, without your additional permission, should you decide to participate in this study.

Will the study have any adverse effects on pregnancy if the patient is pregnant?

Both the DSA and MRI will be done only for a patient who require these studies as part of their treatment or follow up.

There is risk related to ionizing radiation in DSA study which can be harmful to the fetus. Regarding safety of MRI in pregnancy, to date there has been no indication that the use of clinical MRI during pregnancy has produced deleterious effects. However these investigations will be done in a pregnant patient only in situation where the mother's life is in danger and she requires treatment or an immediate follow up study is warranted. For these tests to be done she has to give her informed written consent.

Moreover this study is a comparison of the imaging data from the DSA and MRI tests you have or is about to undergo as part of the treatment. You are not undergoing these tests for the study per se.

If you have any further questions, please ask Dr. Sathish.K (tel: 9400243843) or email: sathisam@sctimst.ac.in

IEC Member Secretary
Dr. Mala Ramanathan
Phone Number : 0471 2524234

CONSENT FORM

<u>TITLE OF THE STUDY:</u> **Imaging of Carotid-Cavernous Fistula – comparing advanced MRI sequences with Digital subtraction angiography**

<u>Study number:</u>

Participant's name: ____

Date of Birth / Age (in years): ________________________________

Son/daughter of ____

(Please tick boxes) •

I declare that I have read the above information provided to me regarding the study – "**Imaging of Carotid-Cavernous Fistula – comparing advanced MRI sequences with Digital subtraction angiography**" -- and have clarified any doubts that I had. [ ]

I understand that my participation in this study is entirely voluntary and that I am free to withdraw the permission to continue my participation at any time without affecting my usual treatment or my legal rights. [ ]

I understand that the study staff and institutional ethics committee members will not need my permission to look at my health records even if I withdraw from the trial. I agree to this access. [ ]

I understand that my identity will not be revealed in any information released to third parties or published [ ]

I voluntarily agree to take part in this study [ ]

I have received a copy of this signed consent form [ ]

Name: ______________________________

Signature:____________________________

Date:________________________________

Name of witness:_______________________

Relation to participant:___________________

Date: _________________________________

(Person Obtaining Consent) I, _______________________________ attest that the requirements for informed consent for the medical research project described in this form have been satisfied. I have discussed the research project with the participant and explained to him or her in nontechnical terms all of the information contained in this informed consent form, including any risks and adverse reactions that may reasonably be expected to occur. I further certify that I encouraged the participant to ask questions and that all questions asked were answered.

______________________________ __________________

Name and Signature of Person Obtaining Consent

Study Title: Imaging of Indirect Carotid-Cavernous Fistula – comparing advanced MRI sequences with Digital Subtraction Angiography

Indirect CCF reporting Format for 3DTOF MRA; SILENT MRA; SWAN and DSA.

a) Reallocated Anonymized Image identification number: ………………………..
b) Study / Sequence evaluated: MRI – (3DTOF MRA ; SILENT MRA;SWAN) /DSA………………...
c) Investigator analyzing study:…………………………… Date of Image analysis:……………
d) Quality of image: four-point scale score*: …………………………………………

Name:
Age:
Sex:
Chief complaints: a.Orbital pain b. Conjunctival injection c. Chemosis d. Proptosis e. Eyelid swelling f. Diplopia g. Ptosis h. Cranial nerve deficits and ophthalmoplegia i. Bruit j. Glaucoma k. Retinal hemorrhage l. Elevated IOP m. Decreased visual acuity n. Seizures o. Intracranial hemorrhage Clinical patterns **-** Orbital pattern **-** Ocular pattern **-** Cavernous pattern **-** Cerebral pattern **-** Mixed

- **MRI parameters:**

1. Lesion side : Right / Left
2. Fistula size (mm)...(CC x TR AP)

TOF:

3. CCF location: ………………………………
4. Arterial Feeders: ICA/ECA…………………
5. Unilateral or bilateral supply …………….
6. Venous drainage: Anterior/ Posterior/Superior/Inferior ………
7. Cortical vein reflux: (Yes/No)………………

Silent:

8. CCF location: ………………………………
9. Arterial Feeders: ICA/ECA…………………
10. Unilateral or bilateral supply …………….
11. Venous drainage: Anterior/ Posterior/Superior/Inferior ………
12. Cortical vein reflux: (Yes/No)………………
13. SWAN - SOV /SSS signal intensity ratio[a]: ……….. Fistulous point ……….. CVR………….

- **DSA parameters:**

a. Lesion side : Right / Left
b. Fistula size (mm)...(CC x TR AP)
c. CCF location
d. Architecture
   Barrow type:
   Suh classification:
e. Feeding artery
f. Unilateral/ bilateral supply …………
g. Venous drainage: Anterior/ Posterior/ Superior/ Inferior ………
h. Cortical venous reflux : Present/absent

Plagiarism Checker X Originality Report

Imaging of Indirect Carotid-Cavernous Fistula – comparing advanced MRI sequences with Digital Subtraction Angiography

Similarity Found: 10%

Date: Sunday, July 28, 2019

Statistics: 1669 words Plagiarized / 15984 Total words

Remarks: Low Plagiarism Detected - Your Document needs Optional Improvement.

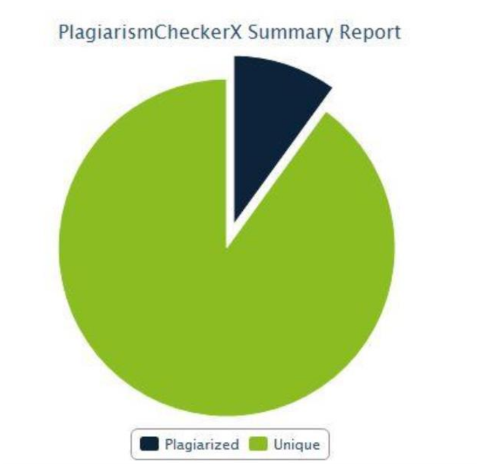

INTERNET SOURCES:

0% - https://www.researchgate.net/profile/Sah
0% - https://link.springer.com/chapter/10.100
0% - http://thejns.org/doi/10.3171/2012.2.FOC
0% - Empty
0% - https://www.wjgnet.com/1949-8470/full/v5
0% - https://link.springer.com/article/10.100
0% - http://www.clevelandclinicmeded.com/live
0% - https://issuu.com/libra64/docs/003987bra
0% - https://sites.google.com/site/dnbstudyma
0% - https://link.springer.com/content/pdf/10
0% - http://www.oired.vt.edu/sanremcrsp/wp-co
0% - https://academic.oup.com/europace/articl
0% - http://pubs.rsna.org/doi/full/10.1148/ra

0% - https://link.springer.com/article/10.100
0% - http://sam.gov/
0% - https://en.wikipedia.org/wiki/Infectious
0% - https://link.springer.com/chapter/10.100
0% - https://www.researchgate.net/publication
0% - https://link.springer.com/article/10.100
0% - https://www.aao.org/eyenet/article/diagn
0% - https://en.wikipedia.org/wiki/Stroke
0% - http://www.neurosurgery.theclinics.com/a
0% - http://www.neuroimaging.theclinics.com/a
0% - https://www.researchgate.net/publication
0% - http://www.sciencedirect.com/science/art
0% - https://radiologykey.com/carotid-caverno
0% - http://www.neurologyindia.com/article.as
0% - http://www.mdpi.com/2079-9721/4/2/19/xml
0% - https://academic.oup.com/qjmed/article/9
0% - https://issuu.com/duvalcountymedicalsoci
0% - http://www.journal-surgery.net/article/S
0% - http://www.medscape.com/medline/abstract
0% - http://thejns.org/doi/pdf/10.3171/2016.5
0% - https://link.springer.com/content/pdf/10
0% - http://www.jefferson.edu/content/dam/tju
0% - http://europepmc.org/articles/PMC3609701
0% - http://thejns.org/doi/10.3171/2016.5.JNS
0% - https://patents.google.com/patent/US5354
0% - https://issuu.com/duvalcountymedicalsoci
0% - http://www.thefoa.org/tech/ref/basic/ter
0% - https://www.everycrsreport.com/reports/R
0% - https://link.springer.com/article/10.100
0% - https://radiologykey.com/neuroradiology/
0% - https://www.wjgnet.com/1949-8470/full/v5
0% - http://www.sciencedirect.com/science/art
0% - http://www.neuroimaging.theclinics.com/a
0% - https://www.wjgnet.com/1949-8470/full/v5
0% - https://link.springer.com/chapter/10.100
0% - http://www.neurosurgery.theclinics.com/a
0% - https://rd.springer.com/content/pdf/10.1
0% - https://www.researchgate.net/publication
0% - https://www.healthline.com/health/head-i
0% - http://www.neuroimaging.theclinics.com/a
0% - https://www.researchgate.net/publication
0% - http://forensicpathologyonline.com/E-Boo
0% - https://link.springer.com/content/pdf/10
0% - http://www.ajnr.org/content/24/9/1789
0% - https://www.wjgnet.com/1949-8470/full/v5
0% - http://www.sciencedirect.com/science/art
0% - http://www.neurosurgery.theclinics.com/a
0% - http://europepmc.org/articles/PMC3380396
0% - http://stroke.ahajournals.org/content/st

MASTER CHART

DSA S.No	AGE	SIDE	LOCATION	NO. OF ARTERIAL FEEDERS	LATERALITY	BARROW	SUH type	ANT-SOV	POST-SPS	INF-IPS	SUP-SMCV	N. OF VEIN	DEEP/BVR	CVR
name001	68	LEFT	1	5	2	D	2	1	0	0	0	1	0	0
name002	61	LEFT	0	5	2	D	2	1	1	1	1	4	1	1
name003	58	LEFT	0	4	2	D	3	1	0	0	0	1	0	0
name004	61	RIGHT	2	5	2	D	2	1	0	0	0	1	0	0
name005	63	LEFT	1	7	2	D	2	1	0	0	0	1	0	0
name006	62	RIGHT	1	2	1	D	3	1	0	0	0	1	0	0
name007	80	LEFT	1	7	2	D	3	1	0	0	0	1	0	0
name008	74	LEFT	1	3	2	C	3	1	0	0	0	1	0	0
name009	53	RIGHT	2	2	1	B	1	0	0	1	0	1	0	0
name010	47	RIGHT	4	10	2	D	1	1	0	1	1	3	1	1
name011	52	LEFT	1	6	2	D	2	1	0	1	1	3	1	1
name012	46	LEFT	4	10	2	D	1	1	0	1	0	2	0	0
name013	57	LEFT	2	3	1	C	3	1	0	0	1	2	0	1
name014	67	RIGHT	1	8	2	D	2	1	0	0	1	2	1	1
name015	65	RIGHT	2	10	2	D	1	1	0	0	1	2	1	1
name016	45	RIGHT	1	6	2	D	3	0	0	0	1	1	0	1
name017	51	LEFT	0	2	1	D	3	1	0	0	1	2	0	1
name018	63	RIGHT	4	4	2	D	2	1	0	0	1	2	0	1
name019	59	LEFT	3	5	2	D	2	1	0	0	0	1	0	0
name020	80	BILATERAL	4	8	2	D	1	0	1	1	1	3	1	1
name021	69	LEFT	1	5	2	D	2	1	0	0	1	2	1	1
name022	58	RIGHT	0	2	1	D	2	1	1	1	0	3	0	0
name023	47	RIGHT	2	4	2	D	1	1	0	1	0	2	0	0
name024	60	BILATERAL	4	6	2	D	1	1	1	1	1	4	1	1
name025	55	LEFT	2	6	2	D	2	1	1	0	0	2	1	1
name026	48	LEFT	3	6	2	D	2	1	1	0	0	2	1	1
name027	46	RIGHT	0	3	2	D	3	1	0	0	0	1	0	0
name028	69	RIGHT	0	3	2	D	3	1	0	0	1	2	0	1
name029	59	BILATERAL	1	8	2	D	1	1	1	1	0	3	0	0
name030	45	LEFT	2	7	2	D	1	1	0	0	0	1	0	0
name031	58	LEFT	1	7	2	D	1	1	1	1	1	4	1	1
name032	61	LEFT	1	7	2	D	1	1	0	1	1	3	1	1
name033	61	RIGHT	3	4	1	D	2	0	1	0	0	1	1	1
name034	48	RIGHT	3	7	2	D	1	1	0	0	1	2	1	1
name035	67	RIGHT	1	6	2	D	1	1	1	0	1	3	1	1
name036	74	LEFT	1	10	2	D	1	1	0	1	1	3	1	1
name037	65	RIGHT	2	7	2	D	1	0	0	0	1	1	1	1

TOF S.No	AGE	SIDE	LOCATION	NO. OF ARTERIAL FEEDERS	LATERALITY	BARROW	SUH type	ANT-SOV	POST-SPS	INF-IPS	SUP-SMCV	N. OF VEIN	DEEP/BVR	CVR
name001	68	LEFT	1	5	2	D	2	1	0	0	0	1	0	0
name002	61	LEFT	0	5	2	D	3	1	1	0	1	3	1	1
name003	58	LEFT	0	4	2	D	3	1	0	0	0	1	0	0
name004	61	RIGHT	2	5	1	D	2	1	0	0	0	1	0	0
name005	63	LEFT	1	6	2	D	2	1	0	0	0	1	0	0
name006	62	RIGHT	2	2	1	C	3	1	0	0	0	1	0	0
name007	80	LEFT	1	6	1	D	3	1	0	0	0	1	0	0
name008	74	LEFT	1	3	1	C	3	1	0	0	0	1	0	0
name009	53	RIGHT	2	2	1	B	3	0	0	1	0	1	0	0
name010	47	RIGHT	4	8	2	D	1	1	0	1	1	3	1	1
name011	52	LEFT	1	6	2	D	1	1	0	0	1	2	1	1
name012	46	LEFT	1	8	2	D	1	1	0	1	1	3	0	1
name013	57	LEFT	2	3	1	C	3	0	0	0	1	1	1	1
name014	67	RIGHT	1	5	2	D	2	0	0	0	1	1	0	1
name015	65	RIGHT	2	8	2	D	1	1	0	0	1	2	0	1
name016	45	RIGHT	1	6	2	D	3	0	0	0	1	1	0	1
name017	51	LEFT	0	2	1	D	3	0	0	0	1	1	0	1
name018	63	RIGHT	4	4	2	D	3	0	0	1	1	2	0	1
name019	59	LEFT	3	5	2	D	2	1	0	0	0	1	0	0
name020	80	BILATERAL	3	7	2	D	1	0	1	1	0	2	0	0
name021	69	LEFT	2	5	2	D	2	1	0	0	1	2	1	1
name022	58	RIGHT	0	2	1	D	3	1	0	0	0	1	0	0
name023	47	RIGHT	1	4	2	C	2	1	0	1	0	2	0	0
name024	60	BILATERAL	1	5	2	D	2	1	1	1	1	4	1	1
name025	55	LEFT	2	6	2	D	2	1	1	0	0	2	1	1
name026	48	LEFT	1	6	2	D	2	1	0	0	0	1	0	0
name027	46	RIGHT	0	3	2	D	3	1	0	0	0	1	0	0
name028	69	RIGHT	0	3	2	D	3	1	0	0	0	1	0	0
name029	59	BILATERAL	1	6	2	D	1	1	0	2	0	1	0	0
name030	45	LEFT	2	7	2	D	1	1	0	0	0	1	0	0
name031	58	LEFT	1	5	2	C	1	1	0	1	1	3	1	1
name032	61	LEFT	1	6	2	D	1	1	0	0	1	2	1	1
name033	61	RIGHT	2	4	1	C	3	0	1	0	1	2	0	1
name034	48	RIGHT	2	5	2	D	2	0	0	0	0	0	0	0
name035	67	RIGHT	1	6	2	C	1	1	1	0	1	3	1	1
name036	74	LEFT	1	8	2	D	1	1	0	1	1	3	1	1
name037	65	RIGHT	2	7	2	D	1	0	0	0	1	1	1	1

Silent S.No	AGE	SIDE	LOCATION	NO. OF ARTERIAL FEEDERS	LATERALITY	BARROW	SUH type	ANT-SOV	POST-SPS	INF-IPS	SUP-SMCV	N. OF VEIN	DEEP/BVR	CVR
name001	68	LEFT	1	5	2	D	2	1	0	0	0	1	0	0
name002	61	LEFT	0	5	2	D	3	1	1	0	1	3	1	1
name003	58	LEFT	0	4	2	D	3	1	0	0	0	1	0	0
name004	61	RIGHT	2	5	2	D	2	1	0	0	0	1	0	0
name005	63	LEFT	1	7	2	D	2	1	0	0	0	1	0	0
name006	62	RIGHT	2	2	1	C	3	1	0	0	0	1	0	0
name007	80	LEFT	1	6	2	D	3	1	0	0	0	1	0	0
name008	74	LEFT	1	3	2	C	3	1	0	0	0	1	0	0
name009	53	RIGHT	2	2	1	B	3	0	0	1	0	1	0	0
name010	47	RIGHT	4	8	2	D	1	1	0	1	1	3	1	1
name011	52	LEFT	1	6	2	D	2	1	0	1	1	3	1	1
name012	46	LEFT	1	8	2	D	1	1	0	1	0	2	0	0
name013	57	LEFT	2	3	1	C	3	1	0	0	1	2	1	1
name014	67	RIGHT	1	8	2	D	2	1	0	0	1	2	1	1
name015	65	RIGHT	2	8	2	D	1	1	0	1	1	3	1	1
name016	45	RIGHT	1	6	2	D	3	0	0	0	1	1	0	1
name017	51	LEFT	0	2	1	D	3	0	0	0	1	1	0	1
name018	63	RIGHT	4	4	2	D	2	0	0	0	1	1	0	1
name019	59	LEFT	3	5	1	D	2	1	0	0	0	1	0	0
name020	80	BILATERAL	3	7	2	D	1	0	1	1	0	2	0	0
name021	69	LEFT	2	5	2	D	2	1	0	0	1	2	1	1
name022	58	RIGHT	0	2	1	D	3	1	0	0	0	1	0	0
name023	47	RIGHT	2	4	2	C	2	1	0	1	0	2	0	0
name024	60	BILATERAL	4	5	2	D	2	1	1	1	1	4	1	1
name025	55	LEFT	2	6	2	D	2	1	1	0	0	2	1	1
name026	48	LEFT	1	6	2	D	2	1	1	0	0	2	1	1
name027	46	RIGHT	0	3	2	D	3	1	0	0	0	1	0	0
name028	69	RIGHT	0	3	2	D	3	1	0	0	1	2	0	1
name029	59	BILATERAL	1	6	2	D	1	1	0	1	0	2	0	0
name030	45	LEFT	2	7	2	D	1	1	0	0	0	1	0	0
name031	58	LEFT	1	5	2	D	1	1	0	1	1	3	1	1
name032	61	LEFT	1	7	2	D	1	1	0	1	1	3	1	1
name033	61	RIGHT	3	4	1	C	3	0	0	0	0	0	0	0
name034	48	RIGHT	3	7	2	D	1	1	0	0	1	2	0	1
name035	67	RIGHT	1	6	2	D	1	1	1	0	1	3	1	1
name036	74	LEFT	1	8	2	D	1	1	0	1	1	3	1	1
name037	65	RIGHT	2	7	2	D	1	0	0	0	1	1	1	1

KEYS TO MASTER CHART

Gender:

1-Male

2-Female

Fistula location:

0- Not identified

1- Posteromedial

2- Posterolateral

3- Anterior

4- Midline/ intercavernous sinus

Laterality of feeders:

1. Unilateral

2. Bilateral

Suh’s Type:

1- Proliferative type

2- Early restrictive

3- Late restrictive

Venous drainage:

0-Absent

1-Present

SWAN Brain findings:

0- Absent

1- Present

ABBREVIATIONS

DAVF- Dural Arterio Venous Fistula

CSDAVF- Cavernous sinus dural arteriovenous fistula.

CCF- Carotid cavernous fistula

CT- Computed Tomography

CTA- Computed Tomography Angiography

MRI- Magnetic Resonance Imaging

MRA- Magnetic Resonance Angiography

TOF- Time of Flight

DSA- Digital Subtraction Angiography

SWI- Susceptibility Weighed Imaging

SWAN- Susceptibility Weighed Angiography

ECA- External Carotid Artery

ICA- Internal Carotid Artery

IMA- Internal Maxillary Artery

MMA- Middle meningeal artery

AMA- Accessory meningeal artery

SMCV- Superficial middle cerebral vein

SOV- Superior Ophthalmic Vein

CVR- Cortical Venous Reflux

BVR- Basal vein of Rosenthal

SSS- Superior Sagittal Sinus

SPS- Superior Petrosal Sinus

IPS- Inferior Petrosal Sinus

MIP - Maximum Intensity Projection